ASSESSMENT OF CHANGES IN THE WATER-SURFACE PROFILE OF THE LOWER CANYON OF THE LITTLE COLORADO RIVER, ARIZONA

by

Andrew Franklin Persio

A Thesis Submitted to the Faculty of the

DEPARTMENT OF HYDROLOGY AND WATER RESOURCES

In Partial Fulfillment of the Requirements
For the Degree of

MASTER OF SCIENCE
WITH A MAJOR IN HYDROLOGY

In the Graduate College

THE UNIVERSITY OF ARIZONA

2004

STATEMENT BY AUTHOR

This thesis has been submitted in partial fulfillment of requirements for an advanced degree at The University of Arizona and is deposited in the University Library to be made available to borrowers under rules of the Library.

Brief quotations from this thesis are available without special permission, provided that accurate acknowledgement of the source is made. Request for permission for extended quotation from or reproduction of this manuscript in whole or in part may be granted by the head of the major department or the Dean of the Graduate College when in his or her judgment the proposed use of the material is in the interests of scholarship. In all other instances, however, permission must be obtained from the author.

Signed:_____

APPROVAL BY THESIS CO-DIRECTORS

This thesis has been approved on the date shown below:

_____ _____

Victor R. Baker — Date
Department Head
Department of Hydrology and Water Resources

_____ _____

Robert H. Webb — Date
Adjunct Associate Professor
Department of Hydrology and Water Resources

ACKNOWLEDGEMENTS

I thank Dr. Robert Webb for support, comments, general guidance through this process, and invaluable field experiences in the Grand Canyon. I would also like to thank Chris Magirl, of the U.S. Geological Survey, for his technical advice and for providing me with Perl scripts to automate long and tedious processes. Peter Griffiths, also of the U.S. Geological Survey, provided the statistical models used in this study as well as, additional technical support. I owe a sincere thanks to Dominic Oldershaw for matching photographs and for participating in the grand adventure that was my field research. I would like to thank my committee members, Drs. Victor Baker and Bart Nijssen, for their support and comments. Mike Breedlove and Tom Gushue, of the Grand Canyon Monitoring and Research Center, provided digital-elevation models and other spatial data which were extremely important to this study. They also generously provided technical assistance with the data itself. I am extremely grateful for funding provided by the U.S. Geological Survey which enabled me to complete and present this research.

TABLE OF CONTENTS

LIST OF TABLES

LIST OF FIGURES

LIST OF APPENDICES

ABSTRACT

The Little Colorado River is the largest tributary of the Colorado River in Grand Canyon and serves as spawning habitat for humpback chub (*Gila cypha*), an endangered species. The lower Little Colorado River, defined as the reach from Blue Springs to the Colorado River, is a dynamic stream, and its channel morphology and longitudinal profile are controlled by several factors, including debris-flow deposition, travertine deposition, and reworking by streamflow floods. I determined changes in the water-surface profile of the Little Colorado River by comparing data surveyed in 1926 by the U.S. Geological Survey and data extracted from 2002 digital-elevation models. Specific changes to the longitudinal profile can be attributed to travertine-dam formation, which appears to occur more quickly than previously assumed; debris-flow deposition; and boulder transport during occasional large mainstem floods. A debris-flow sediment-yield model was used to determine the worst case scenario of boulder inputs from tributaries blocking spawning runs. A one-dimensional steady state flow model shows the effects of changes in channel conveyance on flow velocities in the lower Little Colorado River. Velocity changes associated with debris-flow deposition could potentially affect the ability of humpback chub to move upstream and spawn in this river.

1. INTRODUCTION

The Little Colorado River is the longest tributary to the Colorado River in Grand Canyon, draining 69,800 km^2 of rangeland and forests in northern Arizona and New Mexico (U. S. Department of Agriculture, 1981). The mean annual flow of the Little Colorado River at Cameron, Arizona, is 6.8 m^3/s (Pope and others, 1998). The lower canyon of the Little Colorado River also provides critical habitat for the endangered humpback chub, which live in deep pools near rapids and eddies (Minckley, 1990). The humpback chub move into the warmer waters of the Little Colorado River during the spring and summer months for staging and spawning (Minckley, 1990). This population is the only reproducing population in the lower basin of the Colorado River and is therefore essential to the long-term survival of this endangered fish (Minckley, 1990).

Studies have shown that the river corridors in bedrock canyon rivers, such as the Colorado and Little Colorado Rivers, are not static (Howard and Dolan, 1981). They are shaped by a dynamic interplay between debris flows from tributaries and floods on the mainstem (Graf, 1979; Howard and Dolan, 1981). Debris-flow frequency is linked to tributary morphology, lithology, and climate (Griffiths and others, 2004). The Little Colorado River shares these characteristics with the Colorado River within Grand Canyon and should therefore be affected in the same way.

The purpose of this thesis is to assess the geomorphic changes along the Little Colorado River from Blue Springs to the confluence with the Colorado River between 1926-2002, with special emphasis on predicting the potential effects of debris flows on channel conveyance and morphology. In particular, debris-flow deposition is evaluated using a stochastic model developed for the mainstem of the Colorado River (Webb and

others, 2000). Changes due to naturally occurring debris flows could have important implications for the ability of humpback chub populations to access their spawning reaches, and these implications are assessed in this thesis.

1.1 Previous studies

No previous work has documented debris-flow occurrence in the Little Colorado River or their effects on its longitudinal profile. The U. S. Geological Survey (1927) surveyed a longitudinal profile of the channel to assess the potential for water storage in the lower canyon of the Little Colorado River. They used standard instrumental techniques to survey the longitudinal profile. That 1926 survey provided the baseline for my analysis of changes to the Little Colorado River's water-surface profile. My study is based on work done by Magirl and others (in press), who demonstrated that longitudinal profiles surveyed and determined by remote sensing could be compared. In their work, Magirl and others (in press) compared the 1923 U.S. Geological Survey water-surface profile to one determined by LIght Detection and Ranging (LIDAR) data collected in 2000.

Debris-flow probabilities are based in part on the previous work by Griffiths and others (in press). Their work on Grand Canyon debris-flow occurrence was used as the basis for the probability and frequency models in this study as well as the sediment yield model used in this study. Work done by Webb and others (2000) provided the framework for the debris-flow sediment-yield model.

1.2 Physical Setting

The Little Colorado River is the largest tributary to the Colorado River within Grand Canyon National Park, Arizona (Melis and others, 1996). The Little Colorado

River runs 573 km through northeastern Arizona from its headwaters in the White Mountains of Arizona to its confluence with the Colorado River in Grand Canyon National Park, dropping 1,900 m along the way (Figure 1). The drainage basin covers 56,118 km^2 in northeastern/central Arizona and 13,719 km^2 in northwestern New Mexico. The basin is approximately 394 km long and 254 km wide at its widest point. The mainstem of the Little Colorado River is entirely within Arizona. The basin is bound on the north by the San Juan Basin, to the south by the Gila River Basin, and to the east by the Rio Grande Basin. Mean annual precipitation within the basin is 203-305 mm in the valleys and plateaus and 406–610 mm in the forested highlands (U. S. Department of Agriculture, 1981).

The lower 21 km of the river, which is the study reach, is entirely within a bedrock canyon which contains the same Paleozoic strata as Grand Canyon. At Blue Springs, the Redwall Limestone is at river level forming a narrow channel. At the confluence, the stratigraphy is exposed down to the Tapeats Sandstone. The channel is lined with large boulders reworked from tributary debris fans and occasional travertine accumulations.

The Little Colorado River is ephemeral throughout most of its course. Exceptions include the headwaters and the final 21 km of the river upstream from the Colorado River, which I refer to as the lower Little Colorado River. The lower Little Colorado River is fed by springs discharging out of the Redwall Limestone, primarily Blue Springs (Figure 1). The combined discharge of these springs provides baseflow of ~5.6 m^3/s (Minckley, 1990). The water discharging from these springs contains high levels of calcium carbonate ($CaCO_3$), the source of travertine deposits.

Periodically, large floods occur in the lower Little Colorado River (Figure 2). Most of the largest annual floods have occurred during the fall and winter, 25 and 24 floods, respectively, of the 77 floods on record (Figure 2). Summer monsoons have caused nearly as many of the largest annual floods, (22) as winter and fall. Historically, only six of the largest annual floods have occurred in the spring. The largest historic flood, which occurred in September 1923 (Figure 2), had peak discharge of 3400 m^3/s and occurred shortly after the Birdseye led USGS trip passed the confluence with the Little Colorado River. Flows have been much smaller since the 1923 peak, with a mean annual peak of 297 m^3/s between 1924 and 2003.

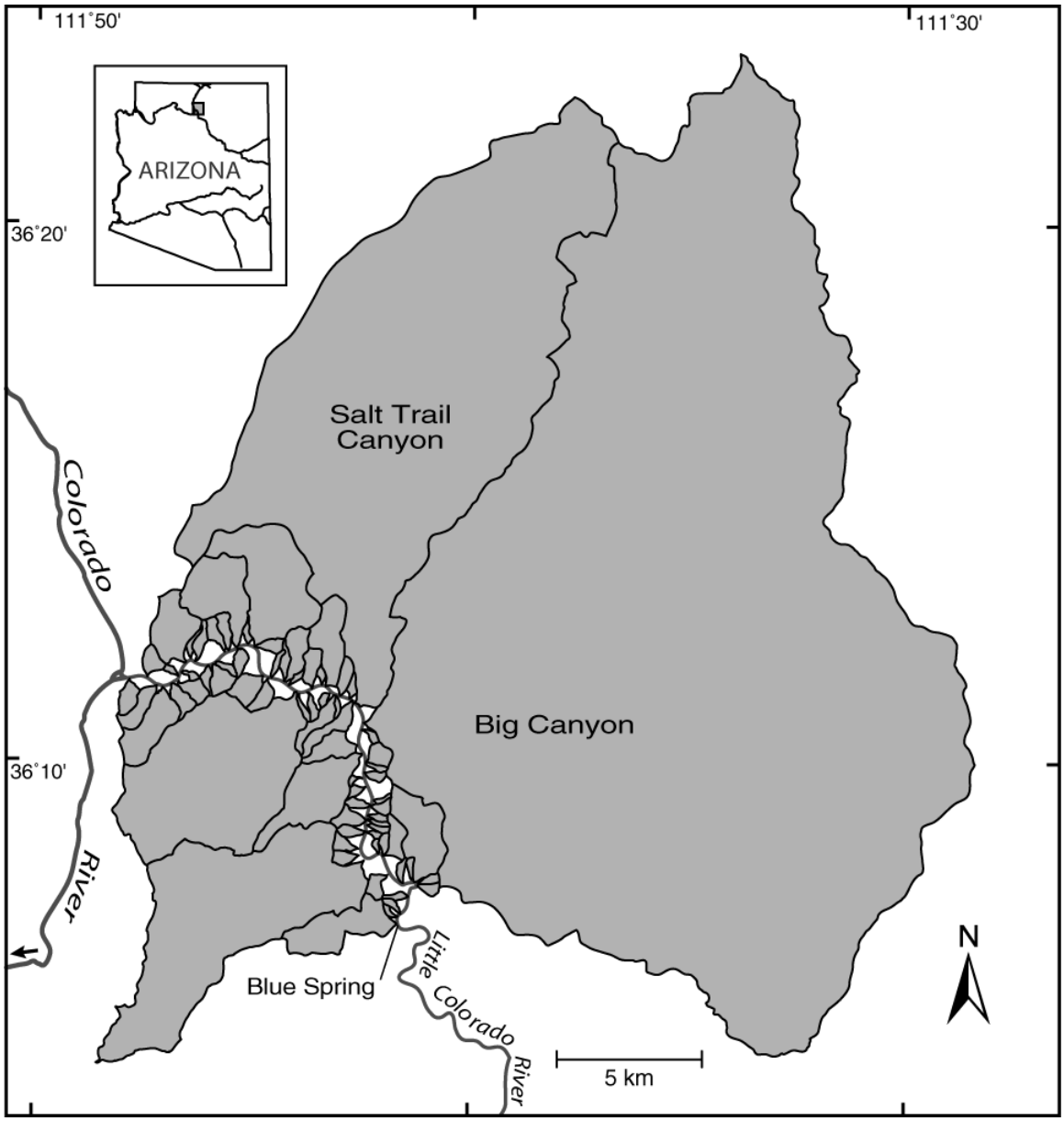

Figure 1. Map of the study area in the lower canyon of the Little Colorado River, Arizona, showing individual drainages.

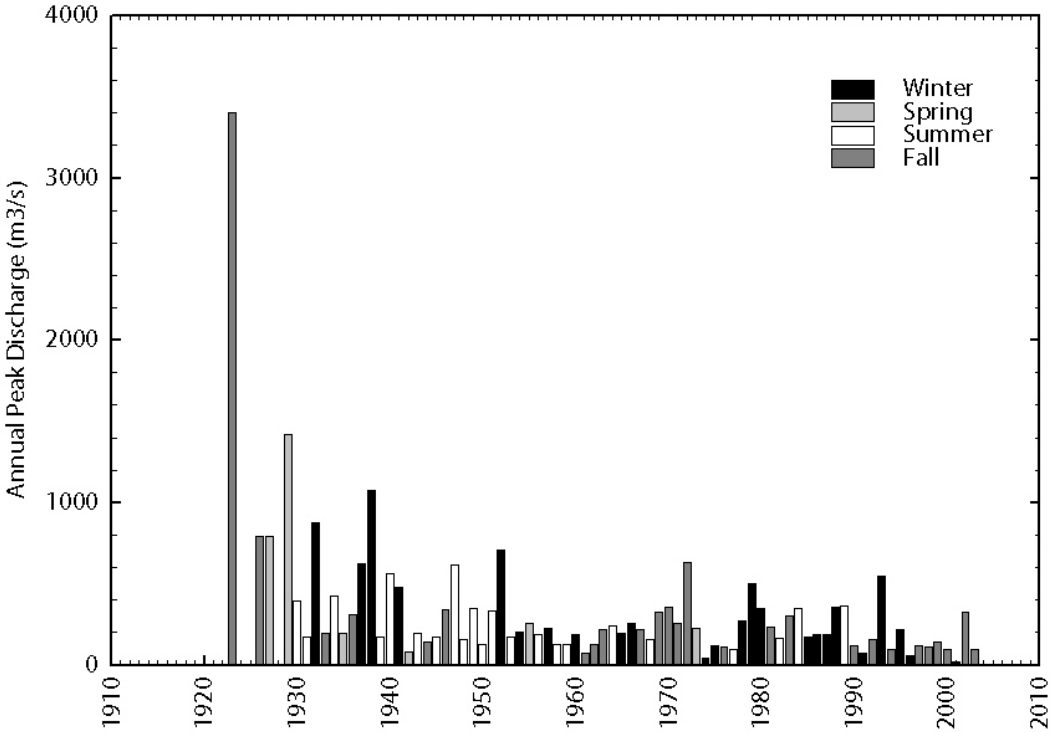

Figure 2. Combined annual flood series for the Little Colorado River at Cameron, Arizona (USGS Gage #09402000), and the Little Colorado River at Grand Falls, Arizona (USGS Gage #09401999). Water years 1926-1946 are from the Grand Falls gauge. Water years 1947-2002 are from the Cameron gaging station.

1.3 Debris flows, travertine, and floods

Debris flows play an important role in supplying coarse sediment to the Colorado River (Webb and others, 2000) as well as its major tributaries within Grand Canyon. Debris flows are sediment-laden flows that have volumetric water contents in the range of 10 to 30% (Pierson and Costa, 1987; Major and Pierson 1992). Unlike avalanches or floods, where the dominate forces are solid-grain forces or fluid forces respectively, debris flows require that these two forces act in concert with one another (Iverson, 1997). They are initiated by several different mechanisms in Grand Canyon and the canyons of the Little Colorado River. The most common mechanism within Grand Canyon is the "firehose effect" (Griffiths and others, 2004). The firehose effect occurs when water pours over the Redwall Limestone or another prominent cliff, onto colluvial wedges, causing slope failures that mobilize into debris flows. Factors that are associated with debris-flow frequency in Grand Canyon include mean height above the river of contributing rock formations, mean slope between the river and contributing rock formations, elevation of the tributary rim, tributary and river aspect, and drainage-basin area (Griffiths and others, in 2004). These parameters are similar in the lower Little Colorado River and therefore debris flows should occur with a similar frequency there. Griffiths and others (2004) have shown that 5.0 debris flows per year occur throughout Grand Canyon, although the frequency in individual tributaries varies widely.

Debris flows have been shown to control channel morphology of the Colorado River (Melis, 1997; Melis and others, 1994; Webb and others, 1989). They contribute to the formation of rapids in Grand Canyon by causing constrictions of the channel as well as delivering large boulders or clusters of boulders to the river (Howard and Dolan, 1981). River reworking removes the smaller boulders, but the largest particles

accumulate to form the core of the rapids.

Another important geomorphic agent in the Little Colorado River is travertine deposition. Travertine is formed where calcium carbonate ($CaCO_3$) precipitates out of river water. The calcium carbonate precipitates as the concentration of $CaCO_3$ reaches the supersaturation point. Precipitation first occurs at the site of microturbulence, such as the river bed and bank obstructions (Giegengack and others, 1979). Initially, the $CaCO_3$ takes the form of tufa, which is a soft form of the mineral; the tufa is then recrystallized to the more resistant travertine (Giegengack and others, 1979). Travertine cements large boulders and other debris together to form large dams and waterfalls in the Little Colorado River (Figure 3). Most of the vertical drop in the lower Little Colorado River is through these waterfalls and dams. Many of these dams are built over existing boulder-controlled rapids.

Large floods also help shape the channel morphology of the Little Colorado River. Periodic floods of a large magnitude can have many effects on the channel morphology (Webb, 1987). Primary effects are the erosion or removal of these large travertine dams and cascades, which can have as much as a 5 m drop (Minckley, 1990). Floods can also shift the channel of the Little Colorado River, as well as remove or deposit gravel and sand bars.

Figure 3. Travertine dam in the lower canyon of the Little Colorado River, Arizona.

2. METHODS

2.1 Probability/frequency model

Griffiths and others (2004) developed a logistic-regression model of debris-flow frequency in Grand Canyon between Lee's Ferry and Diamond Creek (river miles 0 to 225.8). Webb and others (2000), using a preliminary frequency model, developed a debris-flow sediment-yield model for Grand Canyon. That model was then adapted for use in the Little Colorado River. The assumption was made that all significant variables remained the same between Grand Canyon and the Little Colorado River. This is a fair assumption, given that geology, drainage-basin characteristics, and weather are similar between the two localities.

Logistic regression (Hosmer and Lemeshow, 1989) was used to evaluate variables in relation to observed debris-flow occurrence in Grand Canyon between 1890 and 1990, to identify those variables that are statistically significant, and to calculate the probability of debris flow occurrence for each tributary (Griffiths and others, 2004).

Logistic regression predicts the probability of a binomial outcome from continuous, discrete, and (or) binomial independent variables, x. In the case of debris flows in the lower canyon of the Little Colorado River, the outcome is whether or not debris flows will occur during the next one-hundred years in each tributary (yes or no). The independent variables were 20 drainage-basin parameters related to morphometric, climatic, and lithologic characteristics (Griffiths and others, 1996).

With logistic regression, the probability that an event will occur, p(x), is:

$$p(x) = e^{g(x)}/(1+e^{g(x)}) \quad (1)$$

where $g(x) = b_0 + b_i x_i + \ldots + b_n x_n$, i = 1,..., n, and x_i are the variables, b_i are the modeled

variable coefficients, and b_0 is the y-axis intercept (Table 1) (Webb and others, 2000).

Table 1. Variables used to model the probability of debris-flow occurrence in Marble Canyon of the Colorado River in Grand Canyon, Arizona (modified from Griffiths and others, 2004)

Model variables by reach	Units	Variable coefficients[a] b_i
Marble Canyon		
Intercept ($ß_0$)	na	-5.975
Drainage-basin area	log (km^2)	4.675
Height of Hermit Formation	m	-0.014
Gradient below Hermit Formation	deg	0.172
Gradient below Tonto Group	deg	0.180
Drainage-basin gradient	deg	0.184
Height of drainage-basin rim	m	-0.006
River Aspect	none	3.759

Each variable was chosen based on the statistical significance of its contribution to the model (Griffiths and others, 2004). Noteworthy among the significant variables are several terms that reflect the topographic relations of shale-bearing formations to the Colorado River as well as the aspect of the river corridor, which affects how storms interact with canyon walls (Griffiths and others, 1996).

Because of its spatial heterogeneity owing to the pattern of regional geologic structure, Grand Canyon cannot be considered as a single entity when estimating debris-flow probability (Griffiths and others, 2004). Griffiths and others (2004) and Webb and others (2000) divided Grand Canyon into eastern and western modeling reaches for statistical sampling (as opposed to geomorphic) reasons. The data were separated into the large-scale geomorphic reaches of Marble Canyon (river miles 0 to 65), eastern Grand Canyon (river miles 65 to 143), and western Grand Canyon (river miles 143 to 280); the border between Marble Canyon and eastern Grand Canyon traditionally is the mouth of the Little Colorado River (river mile 61.5). A comparison of the sample and population distributions of each drainage basin variable indicates that this division is statistically representative of the population of Grand Canyon tributaries (Griffiths and others, 2004).

The Little Colorado River was modeled using the same variables as the Marble Canyon reach of the Grand Canyon. The conditions in Marble Canyon more closely represent the geomorphic and geologic conditions in the Little Colorado River than those in eastern Grand Canyon. Eastern Grand Canyon has many geomorphic complexities that effect debris-flow occurrence that are not present in the Little Colorado River. The variables that were found to be statistically significant are: drainage-basin area, mean

height above the river of the Hermit Formation, mean slope between the river and the Hermit Formation and Muav Formation, mean slope between the river and the rim of the tributary, mean elevation of the rim of the tributary, and river aspect (Griffiths and others, 2004; Appendix 1).

Following the same procedure developed by Webb and others (2000), I applied their process to the Little Colorado River, converting probability to frequency utilizing a frequency-factor approach similar to that used in traditional flood-frequency analysis (Kite, 1988). The frequency factor, F, is:

$$F = e^{(\mu + K[p(x)] \cdot \sigma)}, \quad (2)$$

where F = expected number of debris flows per century, K [p(x)]= standard normal deviate, and μ and σ are the mean and standard deviation of a lognormal distribution describing all debris-flow frequencies in tributaries of the lower Little Colorado River (Webb and others, 2000).

The values of μ and σ cannot be calculated directly. Instead, values were chosen for μ and s so as to constrain the distribution of F to the known characteristics of debris flows in Grand Canyon: (1) all 736 Grand Canyon tributaries produce debris flows, albeit some at a low frequency (F > 0 for all tributaries); (2) about 60 percent of tributaries produce one or more debris flows per century (F ≥ 1 for 60 percent of tributaries); (3) about 5 percent of tributaries produce 2 or more debris flows per century (F ≥ 2 for 5 percent of tributaries); and (4) no tributary has produced more than 6 debris flows in the last century (F is never greater than 6). The resulting values for μ and s are, μ = 0.95 and σ = 1.75.

2.2 Sediment-yield model

The sediment-yield model used in this study was developed by Webb and others (2000), using updated probabilities presented by Griffiths and others (2004). The model of debris-flow sediment yield in the Little Colorado River involves three distinct elements: (1) frequency and probability models for all 74 tributaries in the lower Little Colorado River that produce debris flows, (2) a model of the expected volumes of debris flows reaching the Little Colorado River, and (3) the particle-size distribution of debris flows. I used the model of maximum volume presented by Webb and others (2000) and updated their model of particle-size distribution.

Debris-flow volumes vary considerably when plotted as a function of drainage area (Webb and others, 2000). It was assumed that, like streamflow floods (Enzel and others, 1993), the volume of sediment delivered by debris flows is a function of drainage area and its upper limit can be described by an enveloping curve of the form:

$$V(A) = a \cdot A^b, \quad (3)$$

where V = total debris-flow volume (m^3), A = drainage area of tributary (km^2), and a and b are empirical coefficients (Webb and others, 2000).

To account for boulder-size particles (b-axis diameter >256 mm), accurate determination of the particle-size distributions using weight-based determinations (e.g., sieve analysis) are problematic because large sample sizes are required. Representative samples of Grand Canyon debris-flow deposits for laboratory sieving cannot be easily collected because of a prohibitively large sample weight. Therefore, several methods were used in combination with sample collection to estimate the particle-size distributions of Grand Canyon debris flows (Webb and others, 2000).

Particle-size distributions were determined by reconstructing the percentage of

particles in each φ (phi) class on the basis of sample weight or by occurrence in point counts. The phi class is defined as $\varphi = -\log_2 D$, where the base of the logarithms is 2 and D is the particle diameter in mm (Allen, 1985). If particle diameters were measured in the field, the particle-size distribution determined using sieve analysis was adjusted for these particles after the particle weight was calculated. If point counts were made on the surface of the deposit from which the sample was collected, the two types of data were combined. Although point counts are made using surface exposure and dry-sieve analyses are based on weight percent of a sample, the order of magnitude of the resulting percentages is similar (Kellerhals and Bray, 1971). It was assumed that point counts accurately measure particle diameters in excess of 64 mm; therefore, the distribution of particles >64 mm was determined using point counts, whereas the distribution of particles <64 mm was determined by combining point count and dry-sieve data. The percentage of particles <64 mm determined by point count was adjusted by the particle-size distribution of the collected sample.

Particle-size distribution for 60 fresh, unaltered debris-flow deposits left by debris flows that occurred between 1965 and 2002 were determined. The deposits are very poorly sorted. Pebbles are the most abundant particles at just over 37 percent by weight. Boulder content is highly variable, but typically accounts for about 18 percent of debris-flow deposits. On average, about 19 percent of all particles are smaller than gravel and particles finer than sand account for only 2 percent of the distribution. The average sand content of debris flows is about 18.2 percent with a range of 2.4 to 47 percent (Webb and others, 2000).

No significant statistical relation was found between sand content and other

factors that might contribute to the high variability, such as drainage area, watershed lithology, or the volume of the debris flow. The highest correlations obtained were between sand-and-finer particles and debris-flow volume ($R^2 = 0.20$) and tributary drainage area ($R^2 = 0.20$). For the sand fraction, alone the highest R^2 value with any variable was 0.04.

The bulk density of debris-flow deposits were estimated using the following equation:

$$\gamma = 2.65 \cdot \sum(W\varphi, \varphi < -1) + 1.50 \cdot \sum(W\varphi, \varphi > -1), \quad (4)$$

where γ = the density of debris-flow deposits and $W\varphi$ = a weight percent fraction for a particle-size range. An average value of $\gamma = 2.4$ Mg/m3 was calculated (Webb and others, 2000).

The expected value of total annual sediment yield by debris flow for a given tributary is estimated as:

$$E[Q_{sdf}] = 0.02 \cdot F \cdot V(A), \quad (5)$$

where $E[Q_{sdf}]$ = the expected value of annual sediment yield from debris flow, F = the frequency factor (the expected number of debris flows per century), V(A) = the maximum (V_{max}) or average (V_{avg}) volume-enveloping curve, and 0.02 is a volume-to-mass and century-to-annual conversion factor (Webb and others, 2000). Debris-flow occurrence varies considerably from year-to-year, both in terms of numbers of events and the volume of sediment delivered. The expected value of debris-flow sediment yield is computed using a conversion factor to convert the frequency information, which has a temporal unit of per century, to an annual unit that is compatible with streamflow sediment yield.

The debris-flow sediment-yield model requires a number of important assumptions. It was assumed that all debris flows from a given tributary are the same size, which means the model does not realistically depict a true magnitude-frequency relation. The sediment-yield model produces an expected value of debris-flow sediment yield; therefore, extreme events not included in the historical record are not accounted for and small events are inadequately represented. Some of these problems could be resolved using a fully stochastic model of debris-flow frequency, but objectively determining model constraints based on the limited data from the ungaged tributaries would be difficult.

2.3 Field investigations

The first goal of field investigations was to determine if debris flows do or do not occur in the lower Little Colorado River. Field investigations were conducted on several occasions. Initial investigations included one day trips from the confluence of the Little Colorado River with the Colorado River scouting for past debris-flow activity. Then in October 2003, I surveyed the reach from Blue Springs to the confluence. During this four-day trip, information was collected to assess the validity of the probability/frequency models as well as the sediment-yield model for use in the Little Colorado River. Data collected included observations of the debris fan activity at tributary junctions, estimated debris-fan size, and estimations of the largest particles on the fan. By comparing the tributary locations with and without debris-flow activity to the models results, I assessed the model's ability to predict debris-flow occurrence in the appropriate locations. Using a similar approach, these observations could also be used to give us a check as to whether the model predicted realistic frequencies.

2.4 Comparison of the 1926 and 2002 water-surface profiles

One of the most important aspects of this study was the comparison of two water-surface profiles. Comparison of these two profiles allowed me to quantitatively measure changes in the water-surface profiles over the 76-year period. The first profile was produced in 1926 by a crew of the United States Geological Survey, using traditional theodolite and stadia rod survey techniques (Birdseye, 1928). The second water-surface profile was generated from 1-m digital-elevation models, provided by the Grand Canyon Monitoring and Research Center. In May 2002, overflights were conducted to collect data for digital-elevation models and ISTAR 4 band digital imagery. The digital-elevation models were created on board using automated photogrammetry airborne GPS, which utilizes internal triangulation from multiple overpasses.

To produce the water-surface profile of the river, the data from the digital-elevation models needed to be processed and analyzed. The first step was to remove all data points that did not fall within the river polygon. The data were then projected from their spatial locations onto a river centerline, constructed by Grand Canyon Monitoring and Research Center, representing the distance along the river relative to the confluence. Once projected onto the centerline, all returns were plotted in an orthogonal format in which elevation values fall on the x-axis and river kilometers fall on the y-axis (Figures 4a and 4b).

Representing elevation returns from all points within the river polygon, the data reflect not only the elevation of the water surface, but also the elevation from the bed of the river and the tops of boulders exposed above the water surface. The water-surface profile was extracted from this relatively noisy “cloud” of data (Figures 4a and 4b). Despite the noise in the data, once analyzed closely, a pattern representing the water

surface became visible. The water surface was interpreted to be the top of the relatively smooth and most dense portion of the “cloud.” The bottom of the “cloud” was interpreted to be the river bottom (Figure 4b). The large excursions in data in the upper 5 km can be explained by the nature of the canyon in this vicinity (Figure 4a). This stretch of river runs through a narrow box canyon and theses excursions represent returns from overhanging cliffs, as well from shadows on the canyon walls.

To account for differences in geographic coordinate systems, both data sets were adjusted in elevation to match the known water-surface elevations at the confluence of the Little Colorado River and the Colorado River. The 1926 water-surface profile was adjusted to the 1923 Birdseye elevation of 827.54 m. The 2002 water-surface profile was adjusted to match the 2000 Lidar-based elevation of 827.77 m (C. Magirl, pers. commun., 2004). Making these two adjustments required the following two assumptions: 1) there has been no change in the water-surface elevation at the confluence between 2000 and 2002 and 2) there was no change between 1923 and 1926. The assumption that there was no change between 2000 and 2002 is probably a safe assumption given that the mainstem discharge was relatively low and there were no large floods from the Little Colorado River during this period. The assumption that there has been no change between 1923 and 1926 is more suspect, considering that the largest historical flood out of the Little Colorado River occurred just after the 1923 survey was completed at the confluence. However, these assumptions were necessary to use the only survey data available to register the two surveys. It would have been beneficial to anchor the two data sets at additional locations where I was confident that no change had occurred over the 76-year period, however no locations met this criterion. Once the two data sets were aligned, they

were directly compared.

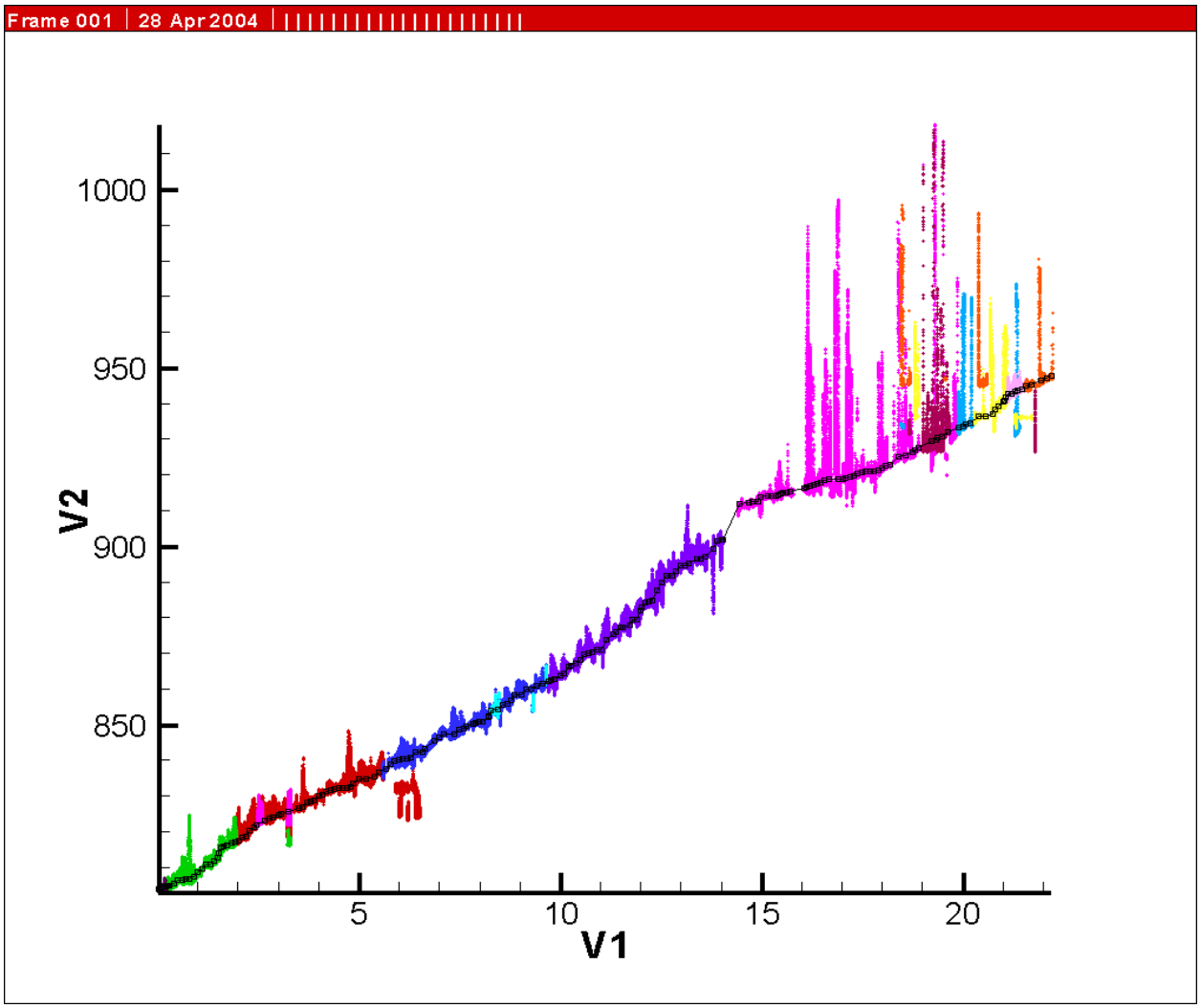

Figure 4a. Figure showing the raw elevation versus river kilometer data. The multicolored data points are the raw data extracted from the digital-elevation models. The black line is the interpreted water-surface profile. Vertical axis is in meters and the horizontal axis is in kilometers.

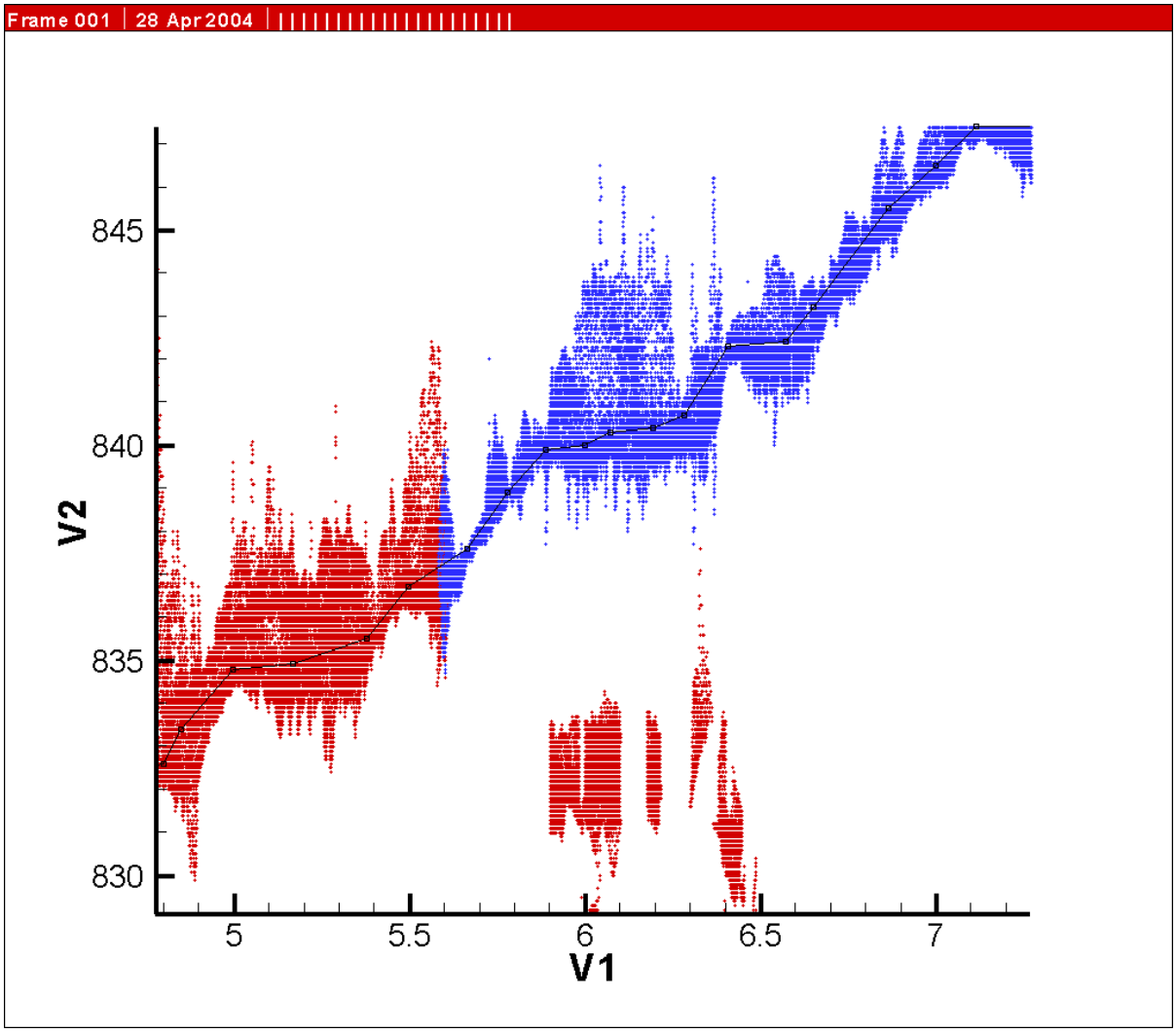

Figure 4b. Figure showing a close up of the raw elevation versus river kilometer data. The multicolored data points are the raw data extracted from the digital-elevation models. The black line is the interpreted water-surface profile. Vertical axis is in meters and the horizontal axis is in kilometers.

2.5 Repeat photography

Repeat photography is a powerful tool for analysis of ecological and geomorphic change. It has been used extensively in the Grand Canyon (Webb, 1996). I utilized repeat photography at Blue Springs to assess geomorphic change there over the last 53 years. Three photos were matched at Blue Springs from originals by Harvey Butchart (1958), Loughlin (1983), and P.W. Hughes (1950). A comparison was also made to photographs taken by Dennis Stone of the Fish and Wildlife Service in June of 1996. The photographs by Stone were not matched exactly because those photographs were obtained after the trip to Blue Springs.

2.6 One-dimensional steady-state flow model

HEC-RAS 3.1 was used to model one-dimensional steady-state flow through the canyon. The model was run as subcritical and the downstream boundary condition was normal depth at the confluence using a downstream slope of 0.0065. This slope was calculated using the simple equation:

$$S = (h_{max} - h_{min})/L$$

where h_{max} is the water-surface elevation at the upstream end of the reach, h_{min} is the water-surface elevation at the confluence, and L is the reach length. Based on visual analyses of the river bed and stream banks I chose Manning's n values of 0.06 and 0.07 respectively.

The cross sections for the model were created from the digital-elevation models by creating a line coverage onto my aforementioned Arc Map (Figure 5). Cross sections were cut where the river's width changed drastically. They were also drawn at the bottom of rapids or riffles, at the top of riffles and then again 0.01 km and 0.03 km above each

rapid or riffle. In all, 652 cross sections were cut in the 21 km reach. Additional data were manually collected for each cross section. These data included river width, the distance to downstream cross section along the left overbank, right overbank, and channel center.

Once the system was analyzed for its current conditions, changes were made at three different tributary junctions to reflect predicted sediment inputs due to debris-flow deposition. The sediment inputs were modeled as triangular wedges with a slope of 0.146. This slope was determined by measuring the slopes of several debris fans in the Little Colorado River and then taking the average. The slopes were measured off of the digital-elevation models. The three selected tributaries are 9, 17, and 41.These three tributaries were chosen because they had probabilities of debris-flow occurrence of 70% or greater as well as predicted sediment yields that were among the 10 greatest volumes. These tributaries were assumed to be the most likely to have significant change over the next 100 years (Figure 6). The model was run with the new aggraded cross-section elevations and comparisons were made between the two model outputs at baseflow conditions. This analysis provided some insight into possible changes in channel conveyance and water-surface profiles due to debris-flow deposition.

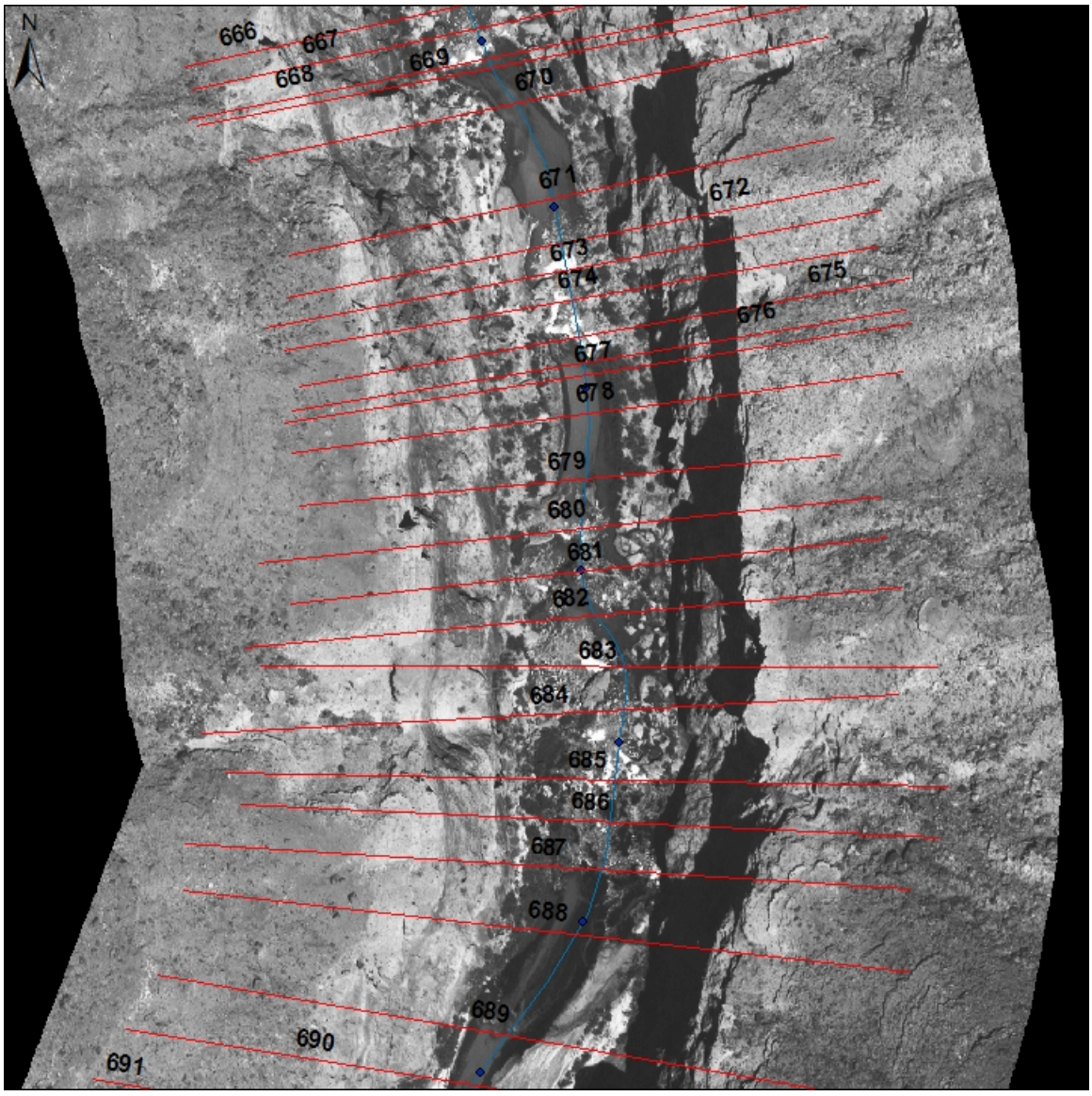

Figure 5. Arc Map image showing the selection of cross sections used for the one-dimensional hydraulic modeling.

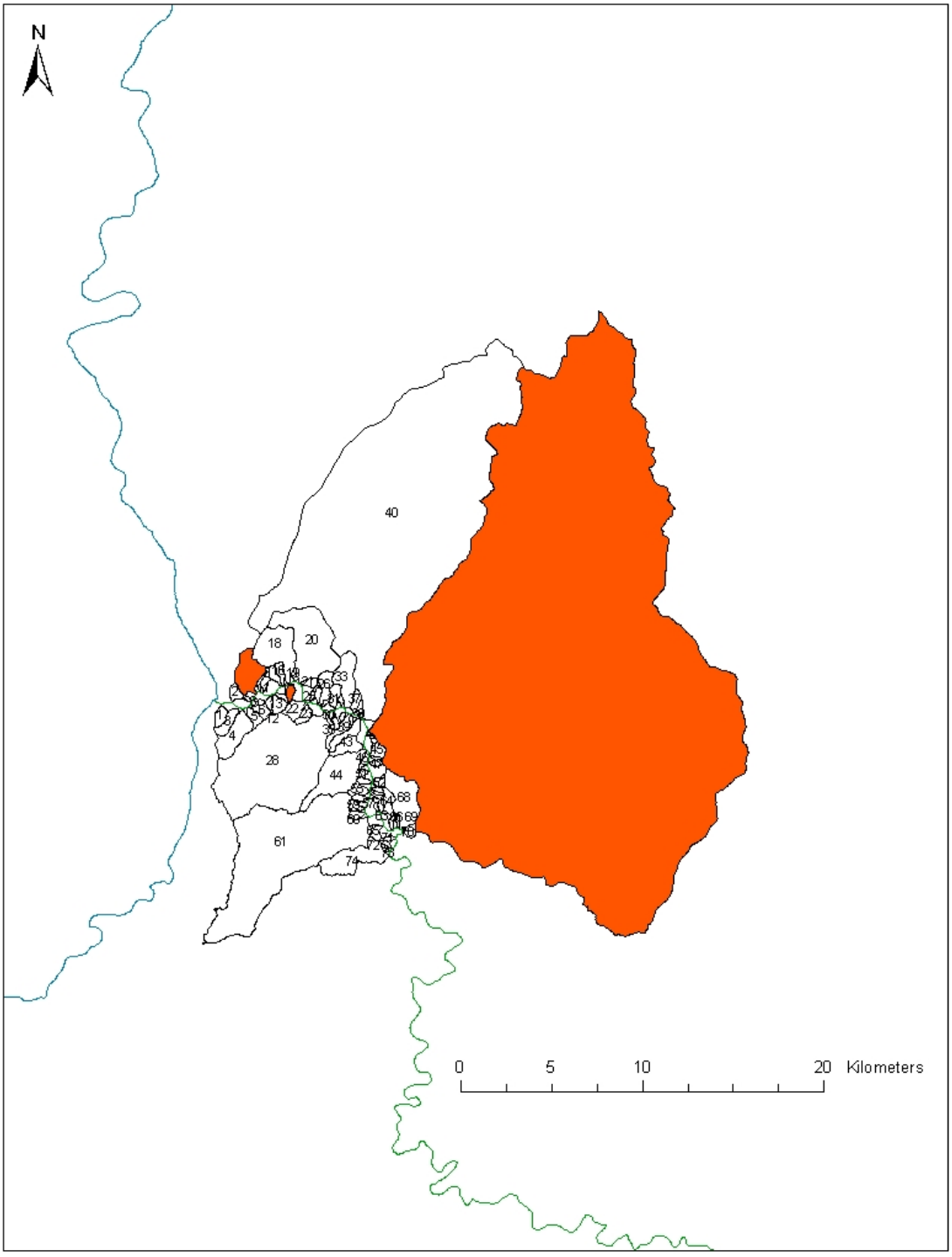

Figure 6. Map showing the locations of tributaries (in red) where the bed surface was raised for HEC-RAS modeling. Numbers indicate the tributary identification number.

3. RESULTS

3.1 Probability/frequency model

Debris-flow deposition could affect several characteristics of the river including, channel morphology, water-surface elevations, and channel conveyance, which could in turn affect the humpback chubs ability to access its spawning grounds. Therefore having realistic probability and frequency models is important. Probabilities of debris-flow occurrence varied considerably between the 74 tributaries within the study reach (Figure 7). The maximum probability of debris-flow occurrence per century was 0.9981, which was predicted for tributary 17, and the minimum probability (0.0003) occurred at tributary 26. The mean probability for the 74 tributaries is 0.2730. See Appendix 1 for a complete listing of each tributaries probability of debris-flow occurrence.

Frequencies of debris-flow occurrence also varied greatly among the 74 tributaries (Figure 8). The highest predicted frequency, at tributary 17, was 5.50 debris flows per century, and the lowest predicted frequency, at tributary 26, was 0.92 debris-flow events per century. The mean frequency for the 74 tributaries is 1.78. See Appendix 1 for a complete listing of tributary frequency values.

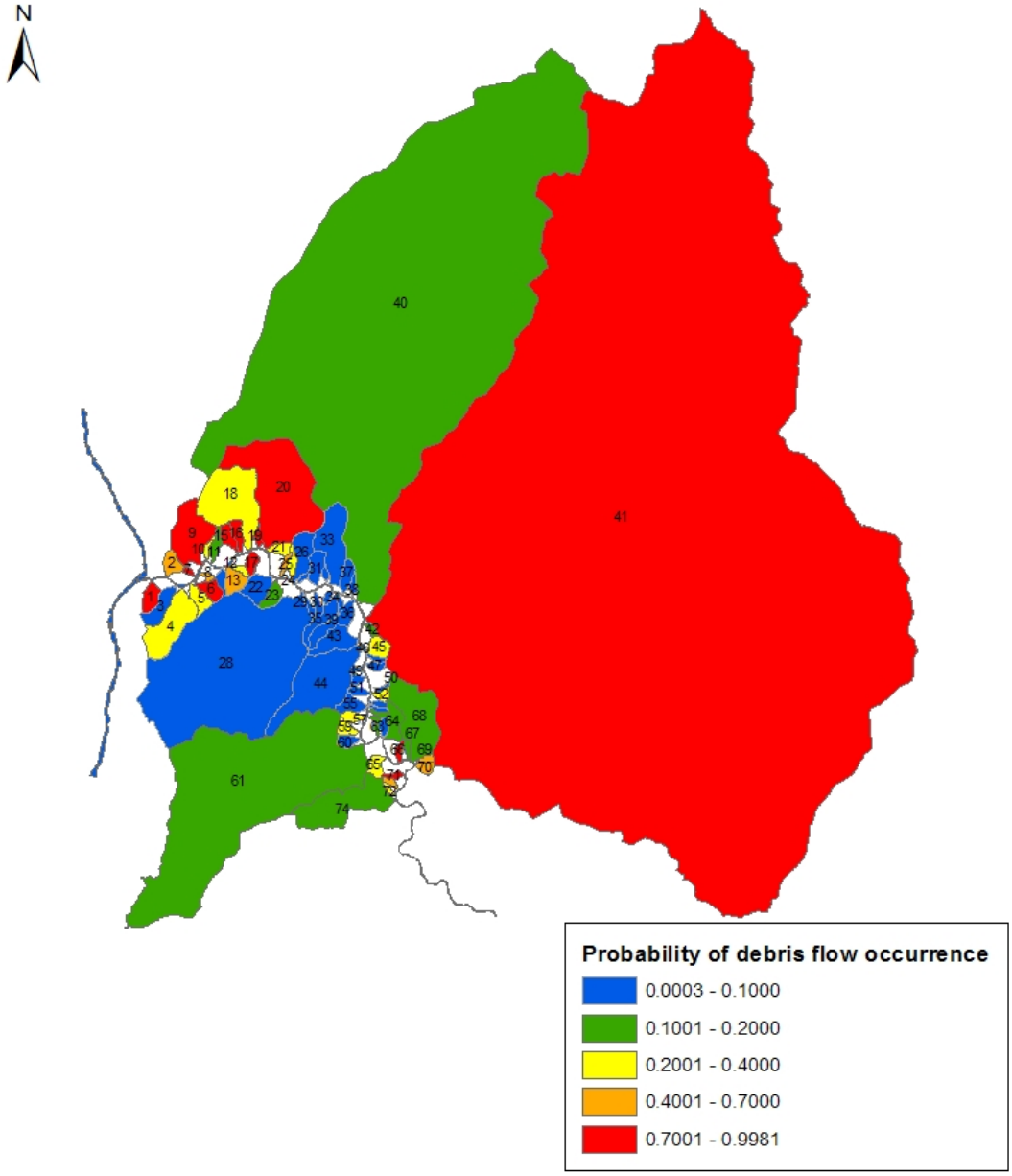

Figure 7. Map showing the probabilities of debris flows occurring out of tributary canyons in the next 100 years. Numbers indicate the tributary identification number.

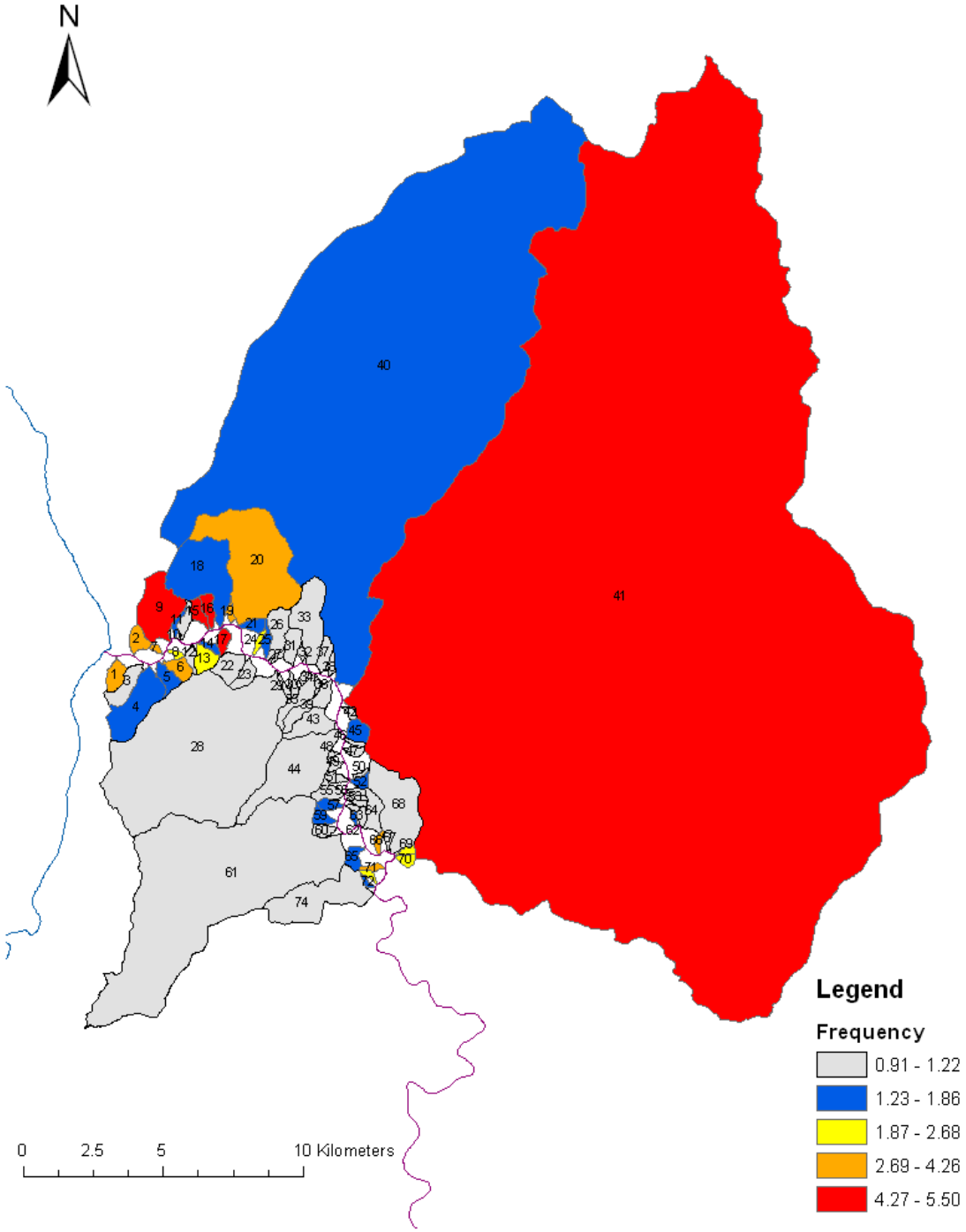

Figure 8. Map showing the predicted frequency of debris-occurrence over a 100-year period. Numbers indicate the tributary identification number.

3.2 Sediment-yield model

The sediment-yield model was used to predict sediment inputs from debris-flow activity out of tributaries. Sediment yields were calculated as a maximum and an average output per tributary over a one-hundred year period. In order to make the sediment-yield data more meaningful in terms of tributaries that could be most effected by debris flows, I also ranked tributaries by the amount of sediment yield predicted divided by the width of the channel at the tributary junction (Figure 9). This analysis could give some insight into which tributaries could see the largest possible changes due to debris-flow activity.

The amount of sediment that each tributary would yield per 100 years was highly variable. Generally speaking, those tributaries with the largest drainage areas had the largest yield. However this was not always the case, since some tributaries with large drainage basins also had low frequencies of occurrence.

The largest sediment inputs are predicted at tributary 41, which has a predicted maximum yield of 68,600 m^3/event. The lowest yield was predicted at tributary 48, which had a predicted maximum yield of 5,570 m^3/event. The mean maximum sediment output for all 74 tributaries is 11,100 m^3 per debris flow.

Tributary 41 at river kilometer 11.4 also had the highest ranking in terms of yield divided by channel width. Tributary 9 at river kilometer 2.9 is ranked number 2 by the same criterion and is therefore the closest tributary to the Colorado River with a high likelihood of significant change due to debris-flow activity (Figure 9). This could have serious implications for the humpback chub if a major debris flow occurred here.

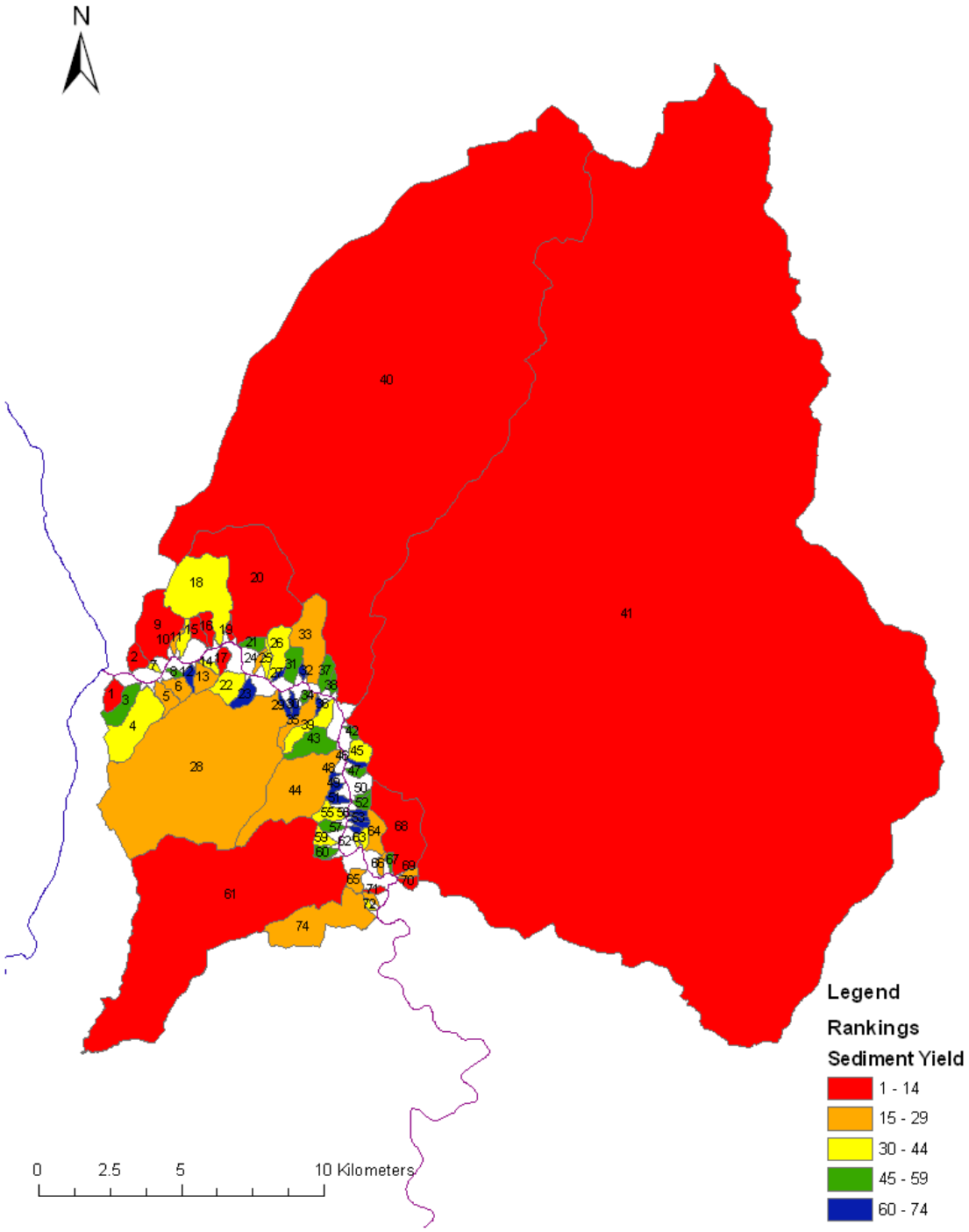

Figure 9. Map showing tributaries ranked by the amount of sediment predicted to be delivered to the river over the course of 100 yrs/channel width at the tributary junction. Numbers indicate the tributary identification number.

3.3 Field investigations

Field investigations show that debris flows are a naturally occurring process in the canyons of the lower Little Colorado River. Evidence of debris flows is present in many of the 74 designated tributaries within the lower 21 km of the Little Colorado River. Of the 74 tributaries delineated in this study, 30 had debris fans or had signs of debris fans that have since been reworked or removed by the river. Most likely there are many more tributaries that have had debris-flow activity but either did not produce debris flows large enough to reach the river or evidence has been eliminated. Many of the tributary mouths in this stretch are perched high above the river on top of the Redwall Limestone, making any real investigation of many tributaries difficult if not impossible from the river.

Ten out of the 19 tributaries with probabilities of debris-flow occurrence greater than 40% had debris fans or showed signs of debris-flow activity. Nine out of those ten had probabilities greater than 70%. Nine out of 17 tributaries with probabilities greater than 70% had signs of recent debris-flow activity. Theses findings lend support to the use of the probability model in the lower Little Colorado River. However, some of the findings from this field work suggest that the model for Grand Canyon may be a bit conservative in its estimates of debris-flow probability in the lower Little Colorado River, alternatively, there may have been an extreme event which removed most of the preexisting debris-flow deposits. For instance, 21 tributaries with evidence of debris-flow activity have probabilities under 40%. Nineteen of those have probabilities under 20%. Furthermore, 4 out of 5 of the tributaries with debris flow related rapids have probabilities under 20%.

Field investigations tended to support the use of the sediment-yield model in the lower Little Colorado River. Evidence of debris-flow activity was discovered at 7 out of

the 10 tributaries with the highest predicted sediment inputs. These 7 tributaries were predicted to have average sediment inputs of greater than 15,000 m^3 per 100 years. Of these tributaries, six had either debris fans or the signs of reworked debris fans. Fifteen tributaries had large fans or showed evidence of large reworked fans; of these, 7 had predicted average sediment inputs of over 10,000 m^3 per 100 years. Two of the tributaries with predicted average sediment inputs of greater than 10,000 m^3 per century did not have debris fans. These two canyons were Salt Trail Canyon and Big Canyon, both of which are relatively large and have perennial flow. It is possible that these two canyons have had significant debris-flow activity in the past but have been completely reworked by a combination of Little Colorado River floods and floods out of their watersheds. There are many large boulders adjacent to the mouth of Big Canyon, which lends some credibility to this hypothesis.

3.4 Comparison of the 1926 and 2002 water-surface profiles

The general trend that appears when comparing the 1926 water-surface profile to the 2002 water-surface profile is that there is aggradation in the first 10 km of the study reach and degradation in the last 12 km (Figure 10 and b). The primary exceptions to this are at river kilometers 14.5 and from river kilometer 21 to 22. There is also approximately 0.9 m of degradation at river kilometer 5.6. Maximum aggradation occurs at river kilometer 2.7, where the 2002 water-surface profile is 5.9 m higher than it was in 1926. Maximum degradation occurs at river kilometer 11.8. The river is 9.9 m lower here than it was in 1926 (Figure 10b).

Although the 2002 water-surface profile is generally lower than the 1926 water-surface profile between river kilometers 10 and 20, there is a sharp rise in elevation

between river kilometer 14.0 and 14.5 which should be considered a significant change from 1926. Between river kilometers 14.03 and 14.47 the 2002 profile shows a rise of over 10 m (Figure 11). This new rise in the water-surface profile is primarily a result of new travertine dams in this area and represents a rise of 2.9 m over the 1926 water-surface profile. Figure 3 shows one of the new travertine deposits in this stretch of river. There is also significant aggradation at Blue Springs, which can be attributed to new debris-flow activity (Figure 12). This will be discussed in more detail in the Repeat Photography section of this report.

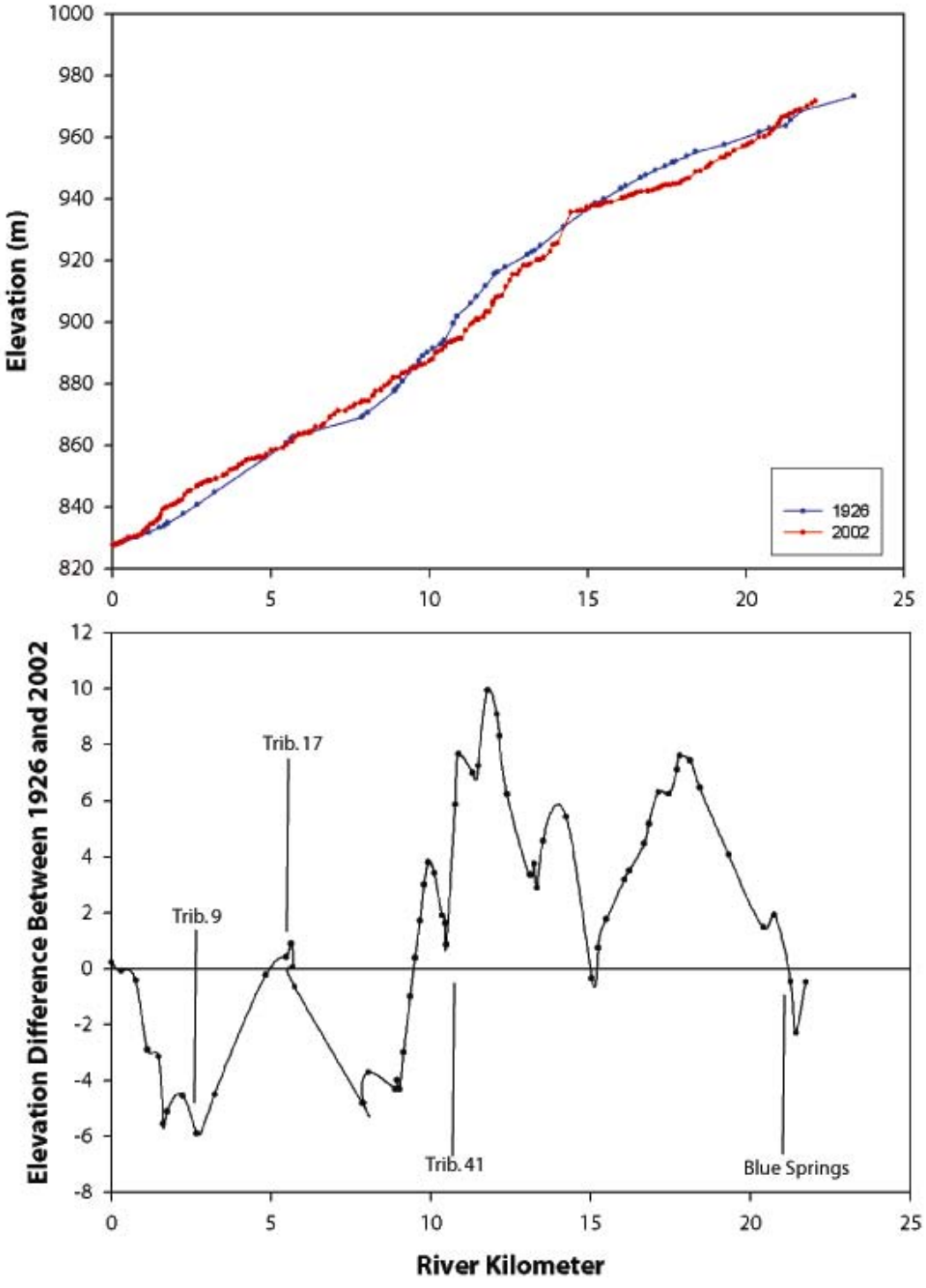

Figure 10a. Comparison of adjusted 1926 and 2002 water-surface profiles.
Figure 10b. Graph showing the elevation difference between 1926 and 2002. Positive values indicate degradation and negative values indicate aggradation.

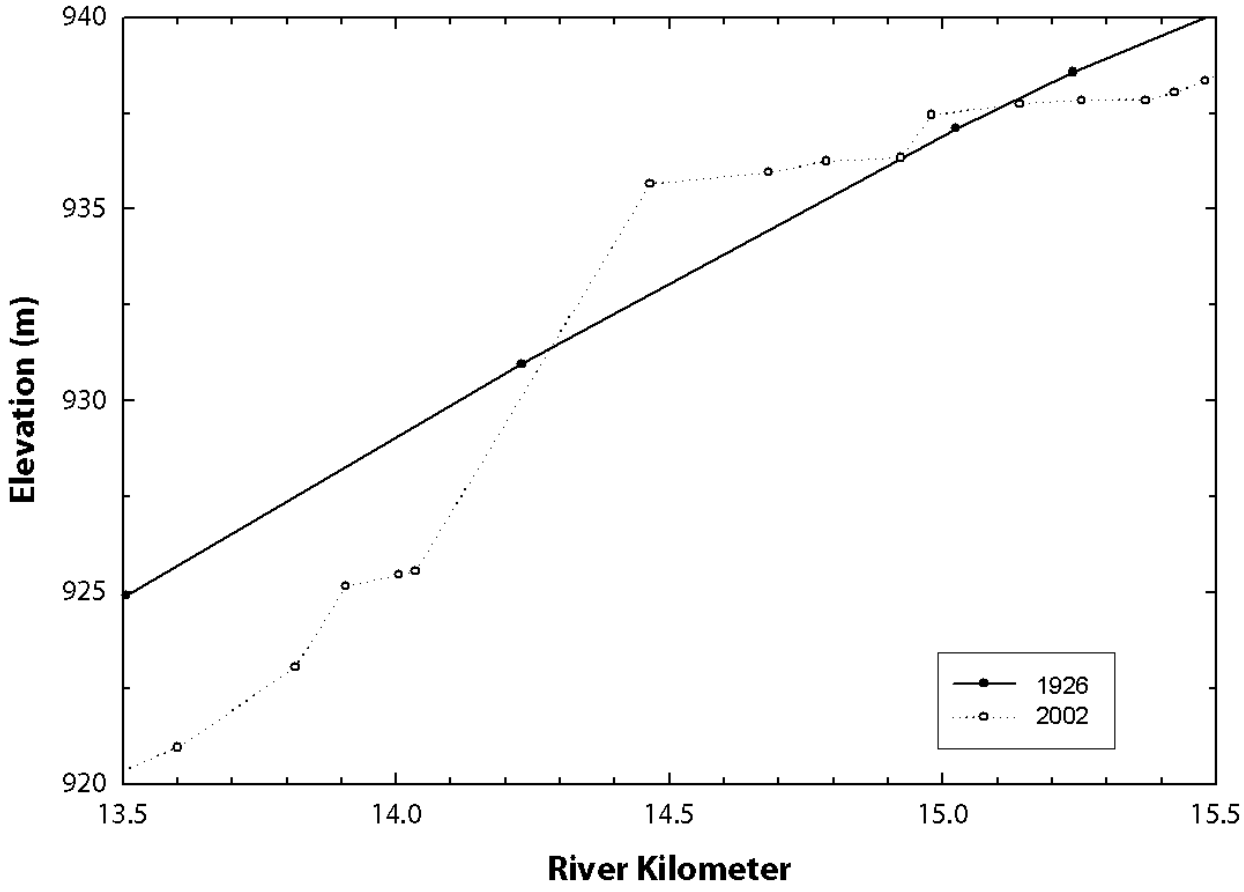

Figure 11. Changes in the water-surface profile at river kilometer 14 between 1926 and 2002.

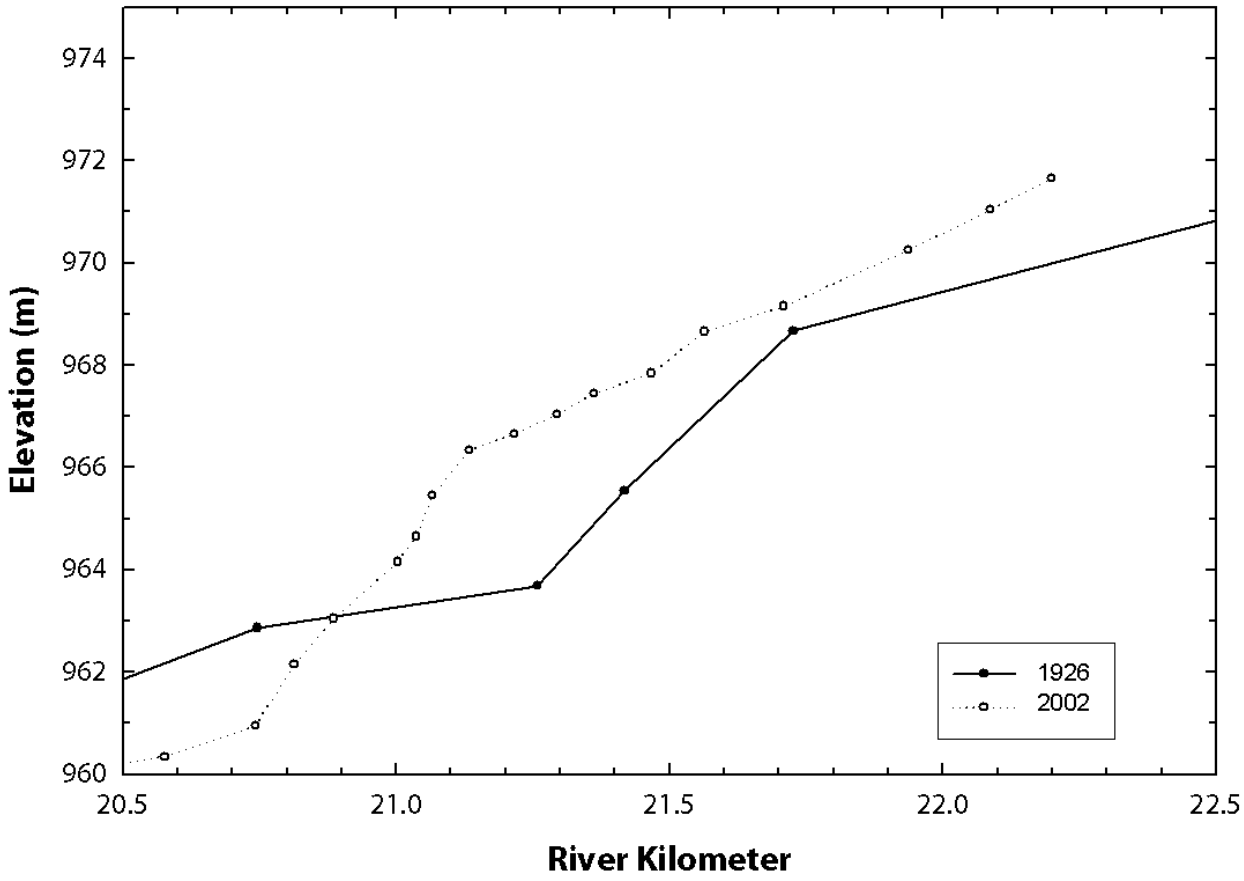

Figure 12. Changes in the water-surface profile at Blue Springs between 1926 and 2002.

3.5 Repeat photography

Repeat photography at Blue Springs yielded some important results. When photos taken by Dennis Stone in June of 1996 were compared to the photos taken by Dominic Oldershaw in October of 2003, several important changes became apparent. The first and most obvious change is that a debris flow occurred sometime between these two dates (Figure 13). Given that there is a significant change in the water-surface profiles at Blue Springs between the 1926 and 2002 profiles (Figure 12), the debris flow must have occurred between June 1996 and May 2002.

The summer of 2001 delivered a lot of rain to the area surrounding the Little Colorado River. It is quite possible that this debris flow occurred during the same rainfall event that contributed to the flooding in Big Canyon on August 8th, which cost photographer George Mancuso his life. Several debris flows in Eastern Grand Canyon occurred during this same time period (Webb and others, 2003).

This debris flow has had several important impacts on the Little Colorado River at Blue Springs. It deposited up to 8 m of new material at the apex of the fan. The resulting debris fan caused a constriction in the river, which along with the deposition of boulders into the river, helped create a steep, rocky rapid adjacent to the fan. Through photo matching I was able to determine that the river has been shifted over to the river right side of the canyon by several meters. The water-surface elevation has also increased here as a result of water pooling up behind the new constriction. The 2002 water-surface profile is 3.3 m higher than the 1926 water-surface profile at river kilometer 21.3, which is just upstream of Blue Springs (Figure 12).

The discharge location of Blue Springs itself has also been altered by the debris-

flow deposition. The springs once discharged at river level just below the rock overhang seen in Figure 13; now the springs discharge out of several locations along the edge of the debris fan as well as upstream of the old discharge location.

Figure 13a. Photograph of Blue Springs taken in June of 1996. Note the springs discharging at river level just below the overhanging rock face. Dennis Stone photograph.

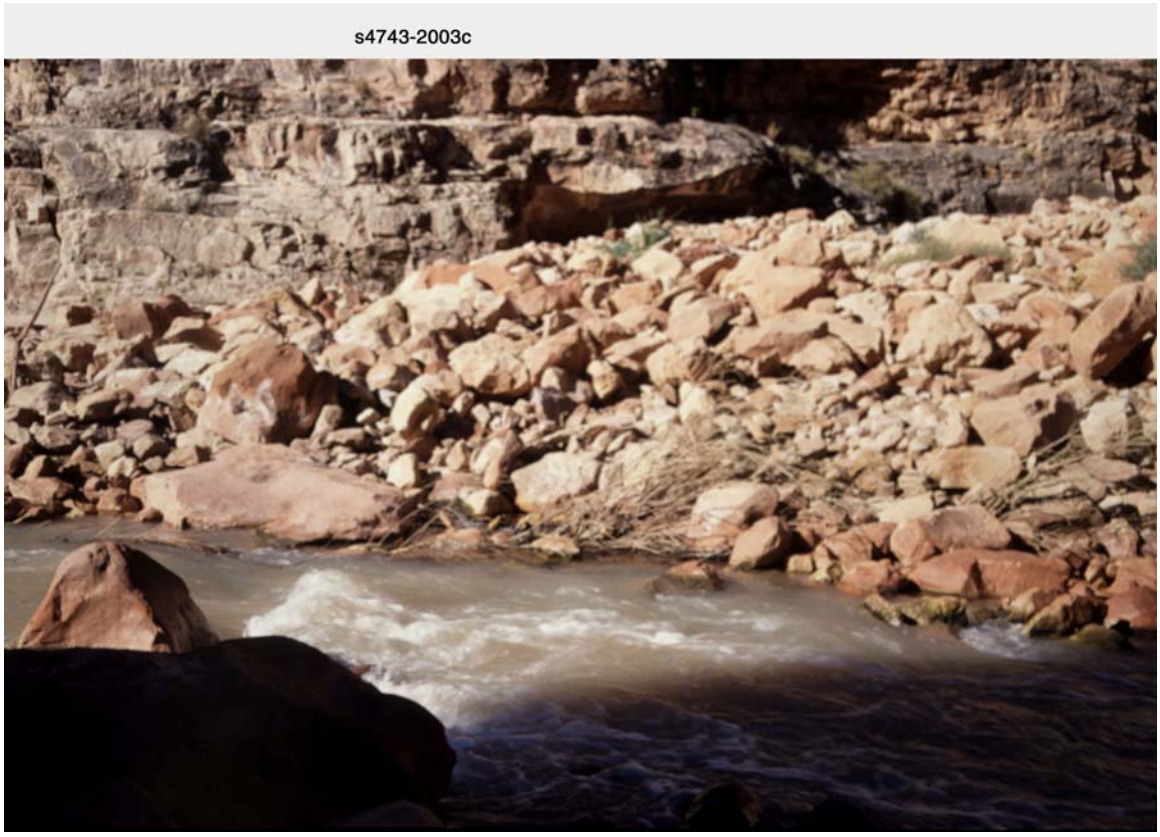

Figure 13b. Photograph of Blue Springs taken in October of 2003. Photograph shows the new debris fan and the resulting changes at Blue Springs. Dominic Oldershaw photograph.

3.6 Effects of debris-flow deposition on flow in the Little Colorado River

I combined the debris-flow sediment-yield model with HEC-RAS modeling to evaluate possible changes in flow velocities at aggraded debris fans. Results show that significant changes would occur at several places, especially at the junction of tributary 41 (Figure 14). At river kilometer 11.28, main channel velocity would increase from 0.69 m/s to 2.05 m/s, and the water-surface elevation would rise 1.36 m, increasing from 875.06 m to 877.43 m elevation. Water would pond behind the newly aggraded fan as far upstream as river kilometer 11.65. In contrast, the junction of tributary 17 and the Little Colorado River would remain almost unaffected as sediment inputs would most likely be deposited upslope of the main channel. Small changes in both velocity and water-surface elevation would occur at the junction of tributary 9 at river kilometer 2.9 (Figure 14). Channel velocity would increase by 0.92 m/s and the water-surface elevation would increase by 0.49 m at the same location (Table 2).

It is unknown what kind of velocities the humpback chub can swim upstream against. However, changes at tributary 9 and 41 could make it more difficult for these fish to reach their critical spawning grounds. Both of these tributaries are adjacent to reaches of the Little Colorado River which the fish currently utilize. If the changes at tributary 9 were significant enough to impede the upstream travel of the humpback chub, they could have severe consequences to the survival of this endangered fish, because this tributary is approximately 2.5 km upstream from the confluence with the Colorado River; restricting the humpback chub to this small stretch of river may be devastating to the remaining population.

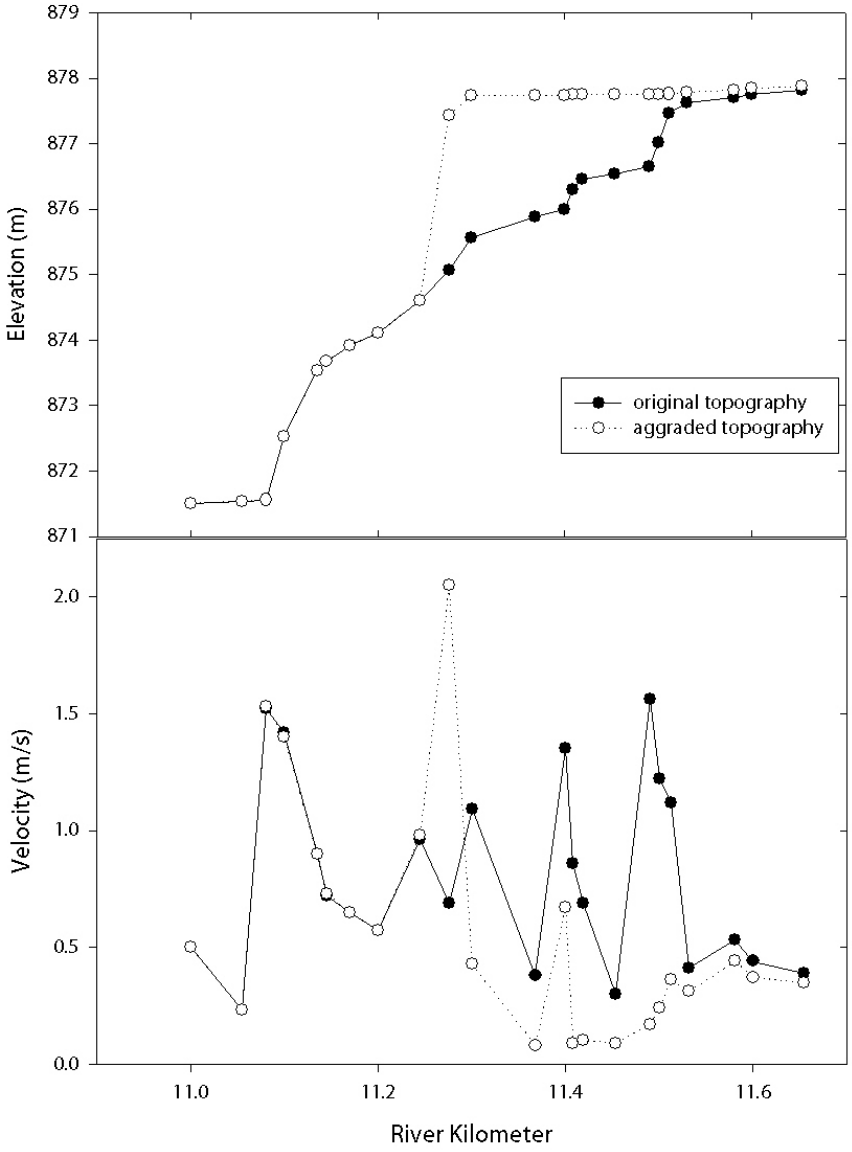

Figure 14. Changes in velocity and water surface elevation due to modeled sediment inputs at river kilometers 11.4 through 11.276.

4. DISCUSSION AND CONCLUSIONS

The Little Colorado River is the largest tributary to the Colorado River in Grand Canyon, and, as such, it plays a critical role in Grand Canyon hydrology and ecology. It provides sediment to the mainstem as well as provides critical habitat for the endangered humpback chub. Based on the results of this study, I predict that significant channel change can result from debris flows on the Little Colorado River within a relatively short period of time. There are many factors which contribute to these changes in addition to debris-flow deposition, including travertine deposition, which appears to occur more quickly than previously assumed; and reworking by streamflow floods. Debris-flow deposition seems to be the most significant factor as it can affect the water-surface profile by increasing fan volumes and channel constrictions, and it also contributes material which often becomes cemented together to form the core of travertine dams.

Dramatic channel change can also occur in a relatively short period of time due to the effects of streamflow floods rapidly eroding travertine dams in the Little Colorado River. Melis and others (1996) documented the rapid erosion of travertine dams in Havasu Canyon, Grand Canyon, Arizona. In his report, he states that among other findings of travertine erosion, one particular travertine waterfall was removed and reformed within a 32-year period. This type of rapid change in travertine deposits could also occur in the lower canyon of the Little Colorado River.

Field investigations show that debris flows are a naturally occurring process in the canyons of the lower Little Colorado River. Field investigations revealed evidence of debris flows in many of the 74 designated tributaries within this reach. Furthermore, field investigations tended to support the use of the sediment-yield model as well as the

probability and frequency models in the lower Little Colorado River. For instance, of the ten tributaries predicted to have the largest sediment inputs, seven had either large debris fans or the signs of reworked debris fans. Ten out of the 19 tributaries with probabilities of debris-flow occurrence greater than 40% had debris fans or showed signs of debris-flow activity. Nine out of those ten had probabilities greater than 70%. Theses findings lend support to the use of the probability model in the lower Little Colorado River. However, some of the findings from this field work seem to show that the model for Grand Canyon may be a bit conservative in its estimates of debris-flow probability in the lower Little Colorado River. For instance, 21 tributaries with evidence of debris-flow activity have probabilities under 40% and 4 out of 5 of the tributaries with debris flow related rapids have probabilities under 20%.

Generally speaking, aggradation occurred historically (1926-2002) in the lower 10 km of the study reach, and degradation occurred in the upper 11 km of the reach. Maximum aggradation occurs at river kilometer 2.7, where the 2002 water-surface profile is 5.9 m higher than it was in 1926. Maximum degradation occurs at river kilometer 11.8, where the river is now 9.9 m lower than it was in 1926 (Figure 10b). The most significant changes occurred at river kilometer 14.5 and at Blue Springs. The increase in water-surface elevation between river kilometer 14.0 and 14.5 was most likely due to a combination of debris-flow deposition and subsequent travertine cementation, resulting in new travertine dams.

The changes at Blue Spring were a direct result of recent debris-flow activity, probably in 2001.The resulting debris fan caused a constriction in the river. The water-surface elevation has increased here as a result of water pooling up behind the new

constriction. The 2002 water-surface profile is 3.3 m higher than the 1926 water-surface profile at river kilometer 21.3.

As the combination of the debris-flow sediment-yield model and one-dimensional flow modeling results show, there is potential for changes in channel velocity that could have serious implications for the survival of the humpback chub. It is unknown what threshold velocity is required to inhibit upstream movement of this endangered species; however, the increase in velocity that I predict could possibly stop upstream movement. The results show that significant changes would occur at several places, in particular, at the junctions of tributaries 9 and 41. At the junction of tributary 41, river kilometer 11.28, main channel velocity would increase from 0.69 m/s to 2.05 m/s, and the water-surface elevation would rise 1.36 m, increasing from 875.06 m to 877.43 m elevation.

Velocity changes at tributary 9 and 41 could make it significantly more difficult for humpback chub to reach their critical spawning grounds. If the changes at tributary 9 were great enough to impede the upstream travel of the humpback chub, they could have severe consequences to the survival of this endangered fish. Since this tributary is approximately 2.5 km upstream from the confluence with the Colorado River; restricting the humpback chub to this small stretch of river may be devastating to the remaining population. The most severe impact to this fish from debris-flow activity would be the complete damming of the river at a location relatively close to the confluence, restricting upstream access. Considering that debris flows do occur in this reach, it is quite possible that one could completely block this small river until it was reworked by a large flood. This would prohibit the humpback chub from reaching a large portion of their spawning grounds as well as greatly reducing the area of their useable habitat.

Future work could include the investigation of why the river is aggrading in the lower reach and why degradation is occurring in the upper reach. Is this phenomenon a result of baselevel aggradation at the confluence of the Little Colorado River and the Colorado River or is it primarily a result of flooding in the Little Colorado River removing material from tributary junctions in the upper reach and redepositing the material in the downstream reach? The island at the confluence could be affecting the aggradation in the lower 10 km of the Little Colorado River by raising the baselevel elevation. These questions could be addressed by further monitoring tributary junctions and the island through repeat photography, as well as continuing to monitor the entire reach through the ongoing collection of DEMs and aerial photographs.

5. REFRENCES

Allen, J.R. L., 1985, Principles of physical sedimentology: Caldwell, New Jersey, Blackburn Press, 272 p.

Birdseye, C.H., 1928, Topographic instructions of the United States Geological Survey, U. S. Geological Survey Bulletin 788, 432 p.

Enzel, Y., Ely, L.L., House, P.K., Baker, V.R., and Webb, R.H., 1993, Paleoflood evidence for a natural upper bound to flood magnitudes in the Colorado River basin: Water Resources Research, v. 29, p. 2287-2297.

Giegengack, R., Ralph, E.K., and Gaines, A.M., 1979, Havasu Canyon – A natural geochemical laboratory, in Linn, R.M. (editor), Proceedings of the first conference on scientific research in the national parks, Vol. II: New Orleans, Louisiana, National Park Service, p. 719-726

Graf, W.L., 1979, Rapids in canyon rivers: Journal of Geology, v. 87, p. 533-551.

Griffiths, P.G., Webb, R.H., and Melis, T.S., 2004, Frequency and initiation of debris flows in Grand Canyon, Arizona, Journal of Geophysical Research: Earth Surface, in press

Hosmer, D.W., and Lemeshow, S., 1989, Applied logistic regression, John Wiley and Sons, New York, p. 307

Howard, A., and Dolan, R., 1981, Geomorphology of the Colorado River in Grand Canyon: Journal of Geology, v. 89, p. 269-297.

Kellerhals, R., and Bray, D.I., 1971, Sampling procedures for coarse fluvial sediments: American Society of Civil Engineers, Journal of the Hydraulics Division, v. 97, p. 1165-1180.

Iverson, R.M., 1997, The physics of debris flows: Reviews of Geophysics, v. 35, p. 245-296.

Kite, G.W., 1988, Frequency and risk analyses in hydrology: Littleton, Colorado, Water Resources Publications, 257 p.

Magirl, C.S., Webb, R.H., and Griffiths, P.G., in press, Changes in the water-surface profile of the Colorado River in Grand Canyon, Arizona between 1923 and 2000, Water Resources Research, in press

Major, J.J., and Pierson, T.C., 1992, Debris flow rheology: experimental analysis of fine-grained slurries: Water Resources Research, v. 28, no. 3, p. 841-858.

Melis, T.S., 1997, Geomorphology of debris flows and alluvial fans in Grand Canyon National Park and their influences on the Colorado River below Glen Canyon Dam, Arizona [Ph.D. Dissertation]: Tucson, University of Arizona, 495 p.

Melis, T.S., Phillips, W.M., Webb, R.H., and Bills, D.J., 1996, When the blue-green waters turn red, historical flooding in Havasu Creek, Arizona: U.S. Geological Survey Water-resources Investigations Report 96-4059, 136 p.

Melis, T.S., Webb, R.H., Griffiths, P.G, and Wise, T.J., 1994, Magnitude and frequency data for historic debris flows in Grand Canyon National Park and vicinity, Arizona: U.S. Geological Survey Water Resources Investigations Report 94-4214, 285 p.

Minckley, W.L., 1990, Native fishes of the Grand Canyon region: An obituary?, in Colorado River ecology and dam management: proceedings of a symposium May 24-25, 1990 Santa Fe, New Mexico, Washington D.C. National Academy Press, p. 124-171.

Pierson, T.C., and Costa, J.E., 1987, A rheologic classification of subaerial sediment-water flows, in Costa, J.E., and Wieczorek, G.F. (editors), Debris flows/avalanches—Process, recognition, and mitigation: Reviews in Engineering Geology, v. 7, p. 1-12.

Pope, G.L., Rigas, P.D., and Smith, C.F., 1998, Statistical summaries of streamflow data and characteristics of drainage basins for selected streamflow-gaging stations in Arizona through water year 1996: U.S. Geological Survey Water Resources Investigations Report 98-4225, 907 p.

U.S. Department of Agriculture, 1981, Little Colorado River Basin, Arizona-New Mexico: summary report, U.S. Department of Agriculture, Washington, D.C., 41 p.

U.S. Geological Survey, 1924, Plan and profile of Colorado River from Lees Ferry, Ariz., to Black Canyon, Ariz.- Nev. and Virgin River, Nev., U.S. Geological Survey, Washington, D.C., 21 sheets

U.S. Geological Survey, 1927, Plan and profile of Little Colorado River from mouth to Tolchico Dam Site, Arizona, U.S. Geological Survey, Washington, D.C., 5 sheets.

Webb, R.H., 1987, Occurrence and geomorphic effects of streamflow and debris flow floods in southern Utah and northern Arizona, in Mayer, Larry, and Nash, D.B. (editors), Catastrophic flooding: Boston, Allen and Unwin, p. 247-265.

Webb, R.H., 1996, Grand Canyon, a century of change, Tucson, University of Arizona Press, 290 p.

Webb, R.H., Griffiths, P.G., and Klearman, T., 2003, Frequency of debris flows in Grand Canyon, U.S. Geological Survey Fact Sheet 065-03, 4 p.

Webb, R.H., Griffiths, P.G., Melis, T.S., and Hartley, D.R., 2000, Sediment delivery by ungaged tributaries of the Colorado River in Grand Canyon, Arizona, U.S. Geological Survey Water-Resources Investigations Report 00-4055, 67p.

Webb, R.H., Pringle, P.T., and Rink, G.R., 1989, Debris flows from tributaries of the Colorado River, Grand Canyon National Park, Arizona: U.S. Geological Survey Professional Paper 1492, 39 p.

Appendix 1. Variables used to model debris flow probability in the lower canyon of the Little Colorado River, Arizona. The resulting probabilities and frequencies of debris-flow occurrence for the next 100 years for each tributary are also listed

Trib-ID	Km	Side	R. Aspect (deg)	Slope (deg)	Hermit Slope (deg)	Muav Slope (deg)	Intercept	Area (log km)	Rim ht. (m)	Hermit ht. (m)	DF Prob.	F
1	0.3	L	269	46	45.84	22.97	-5.975	-0.237	1035	632	0.7507	3.52
2	1.0	R	297	38	39.28	29.97	-5.975	-0.301	625	607	0.6809	3.11
3	1.6	L	307	34	42.89	16.75	-5.975	-0.060	1032	629	0.0175	0.94
4	1.7	L	267	25	44.41	14.67	-5.975	0.423	1033	629	0.2204	1.36
5	2.1	L	235	43	41.54	13.13	-5.975	-0.268	994	628	0.3144	1.61
6	2.2	L	217	45	41.90	20.17	-5.975	-0.268	980	626	0.7169	3.31
7	2.7	R	200	36	0.00	27.86	-5.975	-1.000	465	0	0.8404	4.14
8	2.5	L	194	31	0.00	23.60	-5.975	-0.921	453	0	0.5431	2.42
9	2.9	R	230	39	39.22	40.41	-5.975	0.438	1027	622	0.9977	5.49
10	3.2	R	273	40	41.31	34.62	-5.975	-0.796	992	620	0.2498	1.43
11	3.3	R	315	39	44.66	31.42	-5.975	-0.444	995	620	0.1081	1.11
12	3.8	L	260	41	41.37	11.84	-5.975	-0.638	969	558	0.0626	1.02
13	4.1	L	249	42	41.29	11.04	-5.975	-0.201	969	556	0.4542	2.07
14	4.3	L	230	41	40.73	18.34	-5.975	-0.770	828	556	0.3456	1.70
15	4.6	R	245	37	48.47	30.50	-5.975	-0.398	983	553	0.9344	4.90
16	4.8	R	256	40	42.61	33.71	-5.975	-0.377	981	552	0.9365	4.92
17	4.9	L	238	45	45.01	20.20	-5.975	0.667	1007	587	0.9981	5.50
18	4.9	R	230	12	43.43	35.56	-5.975	-0.481	873	550	0.2219	1.36
19	5.1	R	275	46	46.43	37.67	-5.975	-0.824	966	610	0.8172	3.97
20	5.5	R	295	12	43.18	32.79	-5.975	0.956	997	546	0.8559	4.26
21	5.7	R	305	42	40.87	26.91	-5.975	-0.481	939	546	0.2337	1.39
22	6.7	L	304	40	45.79	6.94	-5.975	-0.056	954	543	0.0858	1.07
23	7.0	L	288	43	42.72	8.53	-5.975	-0.284	934	541	0.1293	1.15
24	7.1	R	278	42	41.21	34.05	-5.975	-0.796	911	539	0.5988	2.68
25	7.4	R	293	35	38.89	33.89	-5.975	-0.553	930	536	0.2728	1.49
26	7.6	R	317	21	40.96	0.00	-5.975	0.013	933	536	0.0003	0.91
27	7.8	R	320	47	47.53	0.00	-5.975	-1.000	855	535	0.0022	0.92
28	8.1	L	309	7	40.06	0.00	-5.975	1.411	1033	472	0.0272	0.96
29	8.2	L	287	37	37.34	0.00	-5.975	-0.796	844	472	0.0016	0.92
30	8.6	L	249	37	42.51	0.00	-5.975	-0.658	876	469	0.0352	0.97
31	8.7	R	244	34	41.79	0.00	-5.975	-0.208	908	530	0.0542	1.01
32	9.0	R	292	44	43.88	0.00	-5.975	-0.921	841	527	0.0040	0.92
33	9.2	R	295	16	43.01	0.00	-5.975	0.400	922	527	0.0048	0.92
34	9.5	L	303	45	41.73	0.00	-5.975	-0.959	771	466	0.0044	0.92
35	9.7	L	293	24	41.10	0.00	-5.975	-0.102	907	526	0.0016	0.92

Trib-ID	Km	Side	R. Aspect (deg)	Slope (deg)	Hermit Slope (deg)	Muav Slope (deg)	Intercept	Area (log km)	Rim ht. (m)	Hermit ht. (m)	DF Prob.	F
36	9.8	L	282	38	35.30	0.00	-5.975	-0.959	831	526	0.0005	0.91
37	10.0	R	295	39	36.64	0.00	-5.975	-0.337	855	463	0.0126	0.93
38	10.5	R	278	36	36.04	0.00	-5.975	-0.770	668	582	0.0013	0.92
39	10.5	L	316	23	37.77	0.00	-5.975	-0.009	904	460	0.0009	0.91
40	10.6	R	318	5	36.05	0.00	-5.975	2.120	1055	457	0.1851	1.27
41	11.2	R	007	6	27.98	0.00	-5.975	2.599	1081	447	0.9148	4.73
42	11.6	R	018	44	41.78	0.00	-5.975	-0.886	718	445	0.1192	1.13
43	12.0	L	349	27	37.46	0.00	-5.975	0.064	882	378	0.0612	1.02
44	12.4	L	314	17	35.43	0.00	-5.975	0.718	881	372	0.0213	0.95
45	12.8	R	358	41	37.50	0.00	-5.975	-0.268	732	427	0.2528	1.44
46	13.0	R	359	38	36.18	0.00	-5.975	-0.921	792	427	0.0051	0.92
47	13.1	R	022	41	39.64	0.00	-5.975	-0.721	798	424	0.0904	1.07
48	13.3	L	352	39	37.63	0.00	-5.975	-1.097	680	363	0.0127	0.93
49	13.6	L	336	43	39.66	0.00	-5.975	-0.796	753	360	0.0431	0.99
50	14.1	R	354	40	32.36	0.00	-5.975	-1.046	759	357	0.0063	0.92
51	14.1	L	001	37	35.99	0.00	-5.975	-0.658	750	354	0.0598	1.02
52	14.3	R	014	42	37.17	0.00	-5.975	-0.620	744	354	0.2942	1.55
53	14.6	R	013	40	37.06	0.00	-5.975	-0.886	736	352	0.0729	1.04
54	14.7	R	003	38	37.02	0.00	-5.975	-0.959	722	351	0.0288	0.96
55	14.7	L	003	26	40.25	0.00	-5.975	-0.301	792	351	0.0679	1.03
56	14.9	R	003	42	39.41	0.00	-5.975	-0.886	733	349	0.1064	1.11
57	15.2	L	003	38	38.84	0.00	-5.975	-0.553	739	346	0.2109	1.33
58	15.2	R	003	43	41.34	0.00	-5.975	-1.046	715	346	0.1022	1.10
59	15.8	L	009	37	39.13	0.00	-5.975	-0.495	744	344	0.2612	1.46
60	16.0	L	331	39	32.89	0.00	-5.975	-0.509	739	343	0.0220	0.95
61	16.2	L	311	13	38.38	0.00	-5.975	1.511	1193	341	0.1594	1.22
62	16.8	R	228	38	34.52	0.00	-5.975	-1.097	523	279	0.1825	1.27
63	16.9	R	293	42	35.04	0.00	-5.975	-0.699	718	279	0.0878	1.07
64	17.1	R	355	25	34.03	0.00	-5.975	-0.143	717	277	0.1180	1.13
65	17.7	L	352	39	34.36	0.00	-5.975	-0.387	718	276	0.3590	1.74
66	18.5	R	226	42	42.72	0.00	-5.975	-0.770	710	274	0.7579	3.57
67	18.7	R	292	46	37.48	0.00	-5.975	-0.886	712	274	0.1358	1.17
68	18.8	R	297	11	37.17	0.00	-5.975	0.585	742	273	0.1225	1.14
69	19.0	R	001	41	41.58	0.00	-5.975	-0.770	685	271	0.4967	2.23
70	19.0	R	007	40	38.06	0.00	-5.975	-0.638	649	268	0.5818	2.60
71	19.3	L	022	41	43.89	0.00	-5.975	-0.824	683	262	0.7218	3.34
72	20.3	L	050	38	40.64	0.00	-5.975	-0.854	680	259	0.5011	2.25
73	20.4	L	031	43	35.97	0.00	-5.975	-1.000	654	258	0.3958	1.86
74	20.7	L	330	14	35.27	0.00	-5.975	0.601	828	255	0.1078	1.11

Appendix 2. Results of sediment-yield model for debris flows in the lower canyon of the Little Colorado River

Tributary-ID	Km	Side	Area (km^2)	Vmax (m^3)	Vavg (m^3)	F	Vavg/100yr	Vavg/yr
1	0.3	L	0.58	10077.96	4931.10	3.52	17366.56	173.67
2	1.0	R	0.50	9645.84	4730.94	3.11	14697.35	146.97
3	1.6	L	0.87	11341.64	5513.85	0.94	5195.55	51.96
4	1.7	L	2.65	15723.29	7509.34	1.36	10190.97	101.91
5	2.1	L	0.54	9851.24	4826.14	1.61	7755.91	77.56
6	2.2	L	0.54	9828.36	4815.54	3.31	15960.97	159.61
7	2.7	R	0.10	6003.15	3021.31	4.14	12502.86	125.03
8	2.5	L	0.12	6316.97	3170.44	2.42	7686.78	76.87
9	2.9	R	2.74	15872.53	7576.72	5.49	41607.83	416.08
10	3.2	R	0.16	6905.88	3449.24	1.43	4935.22	49.35
11	3.3	R	0.36	8742.48	4310.88	1.11	4780.76	47.81
12	3.8	L	0.23	7696.40	3821.47	1.02	3904.62	39.05
13	4.1	L	0.63	10307.49	5037.23	2.07	10409.13	104.09
14	4.3	L	0.17	7038.21	3511.71	1.70	5969.60	59.70
15	4.6	R	0.40	9005.16	4433.26	4.90	21724.39	217.24
16	4.8	R	0.42	9160.41	4505.49	4.92	22165.32	221.65
17	4.9	L	4.64	18540.98	8775.97	5.50	48232.35	482.32
18	4.9	R	0.33	8523.53	4208.72	1.36	5727.04	57.27
19	5.1	R	0.15	6742.12	3371.85	3.97	13384.21	133.84
20	5.5	R	9.04	22554.13	10562.27	4.26	44946.43	449.46
21	5.7	R	0.33	8516.83	4205.59	1.39	5845.66	58.46
22	6.7	L	0.88	11390.86	5536.48	1.07	5898.69	58.99
23	7.0	L	0.52	9733.01	4771.35	1.15	5496.35	54.96
24	7.1	R	0.16	6938.26	3464.53	2.68	9284.87	92.85
25	7.4	R	0.28	8134.01	4026.62	1.49	6004.39	60.04
26	7.6	R	1.03	11916.37	5777.70	0.91	5278.45	52.78
27	7.8	R	0.10	6069.00	3052.64	0.92	2797.96	27.98
28	8.1	L	25.78	30696.30	14136.19	0.96	13554.85	135.55
29	8.2	L	0.16	6874.31	3434.33	0.92	3144.65	31.45
30	8.6	L	0.22	7599.26	3775.85	0.97	3672.96	36.73
31	8.7	R	0.62	10255.17	5013.05	1.01	5045.50	50.45
32	9.0	R	0.12	6263.09	3144.87	0.92	2892.32	28.92
33	9.2	R	2.51	15484.87	7401.62	0.92	6816.26	68.16
34	9.5	L	0.11	6243.73	3135.67	0.92	2885.83	28.86
35	9.7	L	0.79	11032.52	5371.64	0.92	4918.77	49.19
36	9.8	L	0.11	6162.04	3096.87	0.91	2829.93	28.30
37	10.0	R	0.46	9385.77	4610.23	0.93	4306.03	43.06
38	10.5	R	0.17	7068.00	3525.76	0.92	3226.86	32.27
39	10.5	L	0.98	11742.78	5698.08	0.91	5210.68	52.11
40	10.6	R	131.94	49609.90	22257.12	1.27	28349.29	283.49
41	11.2	R	397.57	68612.45	30243.99	4.73	143095.43	1430.95
42	11.6	R	0.13	6549.23	3280.56	1.13	3711.39	37.11
43	12.0	L	1.16	12322.69	5963.81	1.02	6078.70	60.79
44	12.4	L	5.22	19189.88	9066.12	0.95	8600.60	86.01
45	12.8	R	0.54	9833.42	4817.88	1.44	6930.47	69.30
46	13.0	R	0.12	6377.75	3199.28	0.92	2947.96	29.48
47	13.1	R	0.19	7260.31	3616.40	1.07	3884.84	38.85
48	13.3	L	0.08	5569.63	2814.58	0.93	2629.37	26.29
49	13.6	L	0.16	6850.76	3423.20	0.99	3377.33	33.77
50	14.1	R	0.09	5738.59	2895.25	0.92	2673.42	26.73

Tributary-ID	Km	Side	Area (km^2)	Vmax (m^3)	Vavg (m^3)	F	Vavg/100yr	Vavg/yr
51	14.1	L	0.22	7559.33	3757.09	1.02	3819.54	38.20
52	14.3	R	0.24	7736.89	3840.48	1.55	5951.46	59.51
53	14.6	R	0.13	6491.53	3253.22	1.04	3386.37	33.86
54	14.7	R	0.11	6164.53	3098.05	0.96	2978.74	29.79
55	14.7	L	0.50	9659.23	4737.15	1.03	4887.28	48.87
56	14.9	R	0.13	6490.81	3252.88	1.11	3596.57	35.97
57	15.2	L	0.28	8112.88	4016.73	1.33	5358.53	53.59
58	15.2	R	0.09	5780.25	2915.12	1.10	3198.35	31.98
59	15.8	L	0.32	8463.97	4180.91	1.46	6106.30	61.06
60	16.0	L	0.31	8365.56	4134.92	0.95	3927.38	39.27
61	16.2	L	32.41	32834.84	15065.71	1.22	18320.81	183.21
62	16.8	R	0.08	5685.90	2870.11	1.27	3638.26	36.38
63	16.9	R	0.20	7328.63	3648.57	1.07	3900.74	39.01
64	17.1	R	0.72	10718.76	5227.07	1.13	5900.90	59.01
65	17.7	L	0.41	9081.95	4469.00	1.74	7781.35	77.81
66	18.5	R	0.17	7040.02	3512.56	3.57	12532.88	125.33
67	18.7	R	0.13	6513.39	3263.58	1.17	3803.83	38.04
68	18.8	R	3.85	17546.01	8329.99	1.14	9479.42	94.79
69	19.0	R	0.17	7000.67	3493.99	2.23	7793.67	77.94
70	19.0	R	0.23	7648.17	3798.82	2.60	9874.29	98.74
71	19.3	L	0.15	6773.68	3386.77	3.34	11324.64	113.25
72	20.3	L	0.14	6592.14	3300.88	2.25	7421.22	74.21
73	20.4	L	0.10	5958.89	3000.24	1.86	5581.66	55.82
74	20.7	L	3.99	17733.21	8414.00	1.11	9326.40	93.26

Appendix 3. HEC-RAS output for the tributaries where new sediment inputs were modeled.

Original Topography				Aggraded Topography			
Tributary	River Station (km)	W.S. Elev. (m)	Vel. Chnl. (m/s)	Tributary	River Station (km)	W.S. Elev. (m)	Vel. Chnl. (m/s)
41	11.654	877.81	0.39	41	11.654	877.88	0.35
41	11.600	877.75	0.44	41	11.600	877.84	0.37
41	11.581	877.71	0.53	41	11.581	877.82	0.44
41	11.531	877.62	0.41	41	11.531	877.78	0.31
41	11.512	877.47	1.12	41	11.512	877.76	0.36
41	11.500	877.02	1.22	41	11.500	877.75	0.24
41	11.490	876.65	1.56	41	11.490	877.75	0.17
41	11.453	876.54	0.3	41	11.453	877.75	0.09
41	11.419	876.46	0.69	41	11.419	877.75	0.1
41	11.408	876.3	0.86	41	11.408	877.75	0.09
41	11.400	875.99	1.35	41	11.400	877.73	0.67
41	11.368	875.88	0.38	41	11.368	877.74	0.08
41	11.300	875.57	1.09	41	11.300	877.73	0.43
41	11.276	875.06	0.69	41	11.276	877.43	2.05
41	11.245	874.61	0.96	41	11.245	874.6	0.98
41	11.200	874.11	0.57	41	11.200	874.11	0.57
41	11.170	873.92	0.65	41	11.170	873.92	0.65
41	11.145	873.67	0.72	41	11.145	873.67	0.73
41	11.135	873.53	0.9	41	11.135	873.53	0.9
41	11.100	872.52	1.42	41	11.100	872.53	1.4
41	11.081	871.56	1.52	41	11.081	871.56	1.53
41	11.055	871.54	0.23	41	11.055	871.54	0.23
41	11.000	871.51	0.5	41	11.000	871.51	0.5
17	5.407	835.84	0.82	17	5.407	835.85	0.8
17	5.394	835.48	1.25	17	5.394	835.47	1.33
17	5.379	835.42	0.54	17	5.379	835.42	0.54
17	5.367	835.39	0.53	17	5.367	835.39	0.53
17	5.316	835.37	0.25	17	5.316	835.37	0.25
17	5.300	835.36	0.39	17	5.300	835.36	0.39
17	5.296	835.32	0.99	17	5.296	835.32	0.99
17	5.244	835.24	0.4	17	5.244	835.24	0.39
17	5.205	835.19	0.53	17	5.205	835.19	0.53
17	5.200	835.18	0.49	17	5.200	835.18	0.49
17	5.148	835.16	0.27	17	5.148	835.16	0.27
17	5.100	835.14	0.32	17	5.100	835.14	0.32
17	5.045	835.09	0.46	17	5.045	835.09	0.46
17	5.004	834.94	0.72	17	5.004	834.94	0.72
17	5.000	834.87	0.95	17	5.000	834.87	0.94

Original Topography				Aggraded Topography			
Tributary	River Station (km)	W.S. Elev. (m)	Vel. Chnl. (m/s)	Tributary	River Station (km)	W.S. Elev. (m)	Vel. Chnl. (m/s)
17	4.977	834.54	0.55	17	4.977	834.54	0.55
17	4.943	834.08	0.93	17	4.943	834.08	0.92
17	4.913	833.21	1.52	17	4.913	833.21	1.54
17	4.897	832.93	0.91	17	4.897	832.93	0.92
17	4.872	832.9	0.41	17	4.872	832.9	0.41
17	4.854	832.89	0.4	17	4.854	832.89	0.4
17	4.800	832.82	0.45	17	4.800	832.82	0.45
9	3.300	826.62	1.71	9	3.300	826.62	1.73
9	3.243	826.51	0.46	9	3.243	826.51	0.46
9	3.213	826.31	1.42	9	3.213	826.31	1.44
9	3.204	826.21	0.6	9	3.204	826.21	0.6
9	3.168	825.73	1.42	9	3.168	825.73	1.44
9	3.125	825.14	0.7	9	3.125	825.2	0.62
9	3.101	825.09	0.52	9	3.101	825.17	0.46
9	3.049	824.93	0.75	9	3.049	825.02	0.81
9	3.000	824.67	0.72	9	3.000	824.92	0.44
9	2.949	824.44	0.69	9	2.949	824.87	0.4
9	2.900	824.08	0.86	9	2.900	824.57	1.78
9	2.854	823.81	0.56	9	2.854	823.81	0.56
9	2.800	823.66	0.48	9	2.800	823.66	0.48
9	2.759	823.56	0.52	9	2.759	823.56	0.52
9	2.700	823.37	0.58	9	2.700	823.36	0.58
9	2.661	823.2	0.48	9	2.661	823.21	0.47